Universidad de Zaragoza

Departamento de Física de la Materia Condensada

Trabajo Fin de Máster

Strong and Ultrastrong Light-Matter Coupling of Small Quantum Systems near Two-Dimensional Materials

Abstract

We present a full derivation of the coupling between a quantum emitter with two energy levels and the quantized electromagnetic field in media with absorption. This formalism has been applied to a system consisting of an emitter embedded in air in close proximity to a metallic surface. We find out that, by modifying the intrinsic decay rate of the emitter and the distance between, the emitter and the surface the system can reach the strong and even the ultrastrong coupling regime.

Author:
Virginia N. Ciriano

Directors:
Luis Martín Moreno and David Zueco Lainez

28th June 2017

Agradecimientos

Este trabajo no habría sido posible sin la inestimable guía de Luis Martín y David Zueco quienes me han introducido en esta materia desde los principios más básicos. Todo el conocimiento que he obtenido ha sido gracias a sus explicaciones, su paciencia y su buen saber hacer. Asimismo, doy las gracias a Eduardo Sánchez por su buena disposición y ayuda siempre que la he necesitado.

Por otra parte, agradezco al ICMA la financiación recibida para la realización de prácticas externas dentro del programa PI2-ICMA y un contrato de clase GP1 desde el 1 de Mayo.

También quisiera agradecer a mis padres por su apoyo y comprensión así como por haber sido un modelo de trabajo y dedicación a la actividad científica.

Contents

1 Introduction

Light-matter interaction has been studied over the past centuries and our knowledge has grown from the simple observation of the macroscopical ways in which light interacts with matter (absorption, transmission, and reflection)[1] to the understanding of the light wave-particle duality and its quantum mechanics description [2]. The quantized electromagnetic field can be regarded as a sum of excitations, called photons, which have a bosonic character. The branch of optics that studies the phenomena derived from the quantum aspect of the light is called quantum optics. It enables the step from a mere observation of the light to the creation and control of monochromatic light beans thanks to tunable band lasers [3]. At this stage, light was used to study the structure and dynamics of matter since the energy of light lies on the energy range of electronic and vibrational transitions[1].

The development of nanoscience and nanotechnology made necessary the study of optical phenomena on the nanometer scale (nanophotonics). That seemed impossible because the diffraction limit states that there is a maximum to the resolution of any optical system given by nearly a half of the light wavelength (200nm)[1]. However, the diffraction conditions are not applied to a confined field. Therefore, there has been a great effort to find different ways to confine the electromagnetic field.

If light is confined into a small volume and it interacts with only one atom, we can reach new regimes of light-matter interaction, which although possible, are not present in nature. With the development of technology able of reaching temperatures of about 100mK, it was possible to manipulate single atoms and photons [4]. In this context, the atom is pictured as a two level system (TLS) and the electromagnetic (EM) field as a set of quantum oscillators.

Depending on the characteristics of the coupling (strength and dissipation) between one mode of the EM field and the TLS, there are three different regimes: weak, strong and ultrastrong. The regime most common in nature is the weak regime. It is dominated by irreversible losses and shows phenomena such as the spontaneous emission, in which the TLS and EM field interact in an irreversible manner [5]. That is, once the emitter has decayed from the upper to the lower state, the photon emitted does not come back to the TLS.

The strong coupling, on the other hand, is dominated by the strength of the coupling of one EM mode with the TLS. The emitter and the EM mode interchange excitations: the emitter goes from the upper to the lower state creating a photon and this photon is absorbed, exciting the emitter from the lower to the upper state. Because of this interchange of excitations over time, this dynamic is said to be reversible. In this regime, light and matter are entangled, and they cannot be regarded as separated entities anymore [4]. The probability of finding the emitter in the excited state has an oscillating dynamic which decays over time. The frequency of these oscillations, called Rabi oscillations, is related to the strength of the coupling, while the decay time is associated with the dissipation.

The strong regime enable us to use the light not only as an information source, but also as a tool to manipulate atoms [5]. This is why the creation and development of devices capable of

showing strong coupling has been an active line of research. The experiments concerning strong coupling and its applications in the creation of quantum bits made S. Haroche and D. Wineland be awarded with a Nobel prize in 2012. Since then, strong coupling has been achieved in some systems as quantum dots, photonic crystals, superconducting circuits...

If the frequency of Rabi oscillations, related to the strength of the coupling, is of the same order of magnitude as the light frequency, we arrive at the so called ultrastrong coupling. This regime shows a new physics never seen before. However, it is extremely difficult to achieve for traditional quantum optics (cavities QED, ion traps..)[6]. The experiments that have accomplished an ultrastrong light-matter interaction involve many atoms [7] or a superconducting circuit acting as an artificial atom [8] with a giant effective dipole moment.

Besides its relevance in fundamental research, strong coupling has many applications. It can be used to detect single atoms [9], to modify the "chemistry" of the excited levels and to control chemical reactions rate via quantum light [10]... Nevertheless, one of the most relevant features of strong coupling is that it is a necessary condition for quantum information processing [6]. This is because, due to frequency and decay of Rabi oscillation can be totally determined for a given environment, strong coupling can be used to initialize an emitter, which acts as a qubit, in its excited or ground state. Moreover, it would be possible the implementation of a quantum networks, consisting in many quantum nodes (Cavities QED acting as qubits) connected coherently through photons [11]. The quantum information would be generated, processed, and stored in a node (cavities) and it would be transferred to another node via a photon entangled to that atom in the node.

In this work we study the conditions to arrive at the strong and ultrastrong regime for one single atom embedded in the air near to a metallic surface. The interface produces hybrid modes formed by electron oscillations in the metal and electromagnetic oscillations in the dielectric which propagate along the metallic surface. These electromagnetic modes are tied to the metallic surface, providing a field confinement which is required to enter into the strong and ultrastrong regime. We study the interaction for two metals: silver and gold.

The work is organized as follows. We first introduce in Sec.3 a formalism to quantize the electromagnetic field in dispersive and absorbing media within a Green's function approach. In Sec.4 this formalism is applied to find the interaction between the electromagnetic field and an emitter. We continue evaluating the coupling in the vacuum and in a cavity QED. In Sec.5 . we described light-matter interaction of an atom near to a metallic surface and we showcase our results. In Sec.6 and 7 are presented the summary and conclusions. The details of the calculation are discussed in the appendixes.

2 Goals and Objectives

The main objective of this work was to become introduced into the topic of nanophotonics and, in particular, the understanding of the interaction between an atom and the electromagnetic (EM) field from a quantum point of view. By reading the references presented below:

- I have learnt how to quantize the EM field both in vacuum and in dispersive and absorbing media by using the Huttner and Barnett model.
- I have utilised the Green's function as a useful tool to compute and understand the light-matter interaction.
- I have found out the interaction between an atom and the electromagnetic field from this formalism, and studied the modifications of this interaction in different environments: the vacuum and a cavity QED.

An additional goal was to use the acquired knowledge to study the interaction between an emitter and the electromagnetic field if the emitter is placed in the air but close (2-500nm) to a metallic surface of silver or gold. The tasks carried out have been as follows:

- I have adapted the Huttner and Barnett formalism to the situation of an emitter close to a metallic surface.
- I have computed the coupling (photonic spectral density) between the emitter and the EM modes created in the nearby of the metallic surface beyond the rotational wave approximation. Although I have calculated it for surfaces made of silver and gold, the theory adapted from the Huttner and Barnett model allows to compute how the coupling would be if the properties of a material are known.
- I have recalculated, following [26], the conditions in which we observe the strong coupling regime.
- I have found, for the first time, that an emitter formed by a unique atom near to a metallic surface can reach the ultrastrong coupling.

3 Quantization of the Electromagnetic Field in Dispersive and Absorbing Media

In order to perform a canonical quantization of a given system we need to describe it through a Hamiltonian (or Lagrangian) formalism [12]. Dielectrics, metals or, in general, media with absorption, present losses which, a priori, can not be put in a Hamiltonian way. In a classical theory, these losses are typically introduced in the motion equations phenomenologically, as a negative exponential. Therefore, although Electromagnetic field quantization in vacuum is straightforward [See Appendix A], dispersive and absorbing media need a more careful treatment of the losses to make them compatible with a Hamiltonian formulation.

The origin of absorption can be explained by one example: a dielectric.

A dielectric material is an electric insulator characterized by forming dipoles when an electromagnetic field is applied. In contrast to a conductor, charges cannot freely flow in the material, but they are able to slightly move around their equilibrium position. In this way, they create microscopic dipoles [13]. The effect of these dipoles is macroscopically observed as an electric polarization.

$$\mathbf{P} = \varepsilon_0 \chi \mathbf{E}, \tag{1}$$

where the proportionality constant is the product between the dielectric permittivity of the vacuum ε_0 and the dielectric susceptibility χ.

Along all our work we use **non-magnetic and homogeneous materials** where the magnetic permeability is μ_0 and the electric permittivity, $\varepsilon(\omega) = \varepsilon_0 \cdot \bar{\varepsilon}(\omega)$, is constant within the dielectric.

The constitutive relations of the non-magnetic dielectric of our example are

$$\mathbf{D}(\mathbf{r},\omega) = \varepsilon_0 \bar{\varepsilon}(\omega)\mathbf{E}(\mathbf{r},\omega) \tag{2}$$

$$\mathbf{B}(\mathbf{r},\omega) = \mu_0 \mathbf{H}(\mathbf{r},\omega) \tag{3}$$

and macroscopic Maxwell's equations in SI units, together with the constitutive relations read

$$\nabla \cdot \mathbf{B}(\mathbf{r},\omega) = 0 \tag{4}$$

$$\nabla \cdot \varepsilon_0 \, \bar{\varepsilon}(\mathbf{r},\omega) \, \mathbf{E}(\omega) = \rho(\mathbf{r},\omega) \tag{5}$$

$$\nabla \times \mathbf{E}(\mathbf{r},\omega) = i\omega \, \mathbf{B}(\mathbf{r},\omega) \tag{6}$$

$$\nabla \times \mathbf{B}(\mathbf{r},\omega) = -i\omega\mu_0\varepsilon_0\bar{\varepsilon}(\omega)\mathbf{E}(\mathbf{r},\omega) + \mu_0 \mathbf{j}(\mathbf{r},\omega). \tag{7}$$

Eqs. (6) and (7) imply that the electric field $\mathbf{E}(\mathbf{r},\omega)$ obeys the differential equation

$$\nabla \times \nabla \times \mathbf{E}(\mathbf{r},\omega) - \frac{\omega^2}{c^2}\bar{\varepsilon}(\omega) \, \mathbf{E}(\mathbf{r},\omega) = i\omega\mu_0 \, \mathbf{j}(\mathbf{r},\omega), \tag{8}$$

which in the Fourier Space Eq.(8) reads

$$\boxed{k^2\mathbf{E}(\mathbf{k},\omega) - \frac{\omega^2}{c^2}\bar{\varepsilon}(\omega)\mathbf{E}(\mathbf{k},\omega) = i\omega\mu_0\mathbf{j}(\mathbf{k},\omega)} \tag{9}$$

This equation will be crucial for giving a physical interpretation to our model.

The effect that we seek to describe is dissipation in dielectrics. If an oscillating electric field is applied on the material, the microscopic dipoles will try to rearrange themselves at the field frequency. If the frequency is too high, the dipoles don't have enough time to be rearranged. So that, it arises a delayed between the field and the displacement vector [13]. If we consider the electric field to be harmonic: $\mathbf{E} = \mathbf{E_0}e^{i\omega t}$, the displacement vector shows a phase difference $\mathbf{D} = \mathbf{D_0}e^{i(\omega t+\delta)}$. This delayed gives rise to a complex part of the permittivity through the constitutive relations of the material

$$\varepsilon \mathbf{E_0} = \mathbf{D_0}e^{i\delta}, \tag{10}$$

changing the permittivity to

$$\varepsilon = \varepsilon' + i\varepsilon''. \tag{11}$$

ε' y ε'' can be interpreted as the amount of electric displacement vector that varies, respectively, in-phase and with a $\frac{\pi}{2}$ lag phase with the electric field. Hence, $\varepsilon'' \neq 0$ denotes that the microscopic dipoles of the material are braking, and thus, it represents an energy loss.

Having a complex permittivity, a propagating electric field in the z direction is:

$$\mathbf{E} = \mathbf{E_0}e^{i(\omega t - \sqrt{\varepsilon_r' + i\varepsilon_r''}k_0 z)}. \tag{12}$$

Exactly as in the harmonic oscillator, losses are modelled by a negative real exponential in the solution. This phenomenological model is characterized for including the dissipation with a term $-\gamma\dot{x}$ in the motion equation, being γ the viscosity and $\dot{x}$ the oscillator velocity. Unfortunately, this term added *ad hoc* cannot be included in a Hamiltonian formalism .

3.1 Bath Model

In order to include the losses in a dielectric within a quantum mechanical compatible formulation we use a reservoir (or bath) formed by an infinite set of oscillators coupled to the electromagnetic field [14]. Because of the degree of freedom of the bath is infinite, this coupling produces an irreversibility in the flow of energy (and information) from the EM field to the bath. So that, it looks like the EM is loosing energy.

The model can be pictured as follows. At each point of the dielectric we have an electric field **E(r)** coupled with an infinite set of oscillators, each one with a different frequency. It is like at each position we had an infinite set of invented modes that interact with the EM field. Fig.(1) presents a vision of the reservoir oscillators.

The Lagrangian has three terms: a part from the electromagnetic field, another from the reservoir and one last part taking into account the interaction between them. This last term comes from the Huttner and Battner model of the EM field quantization in dielectrics [14]. Thus,

$$L_{total} = L_{EM} + L_{Bath} + L_{int} \tag{13}$$

with

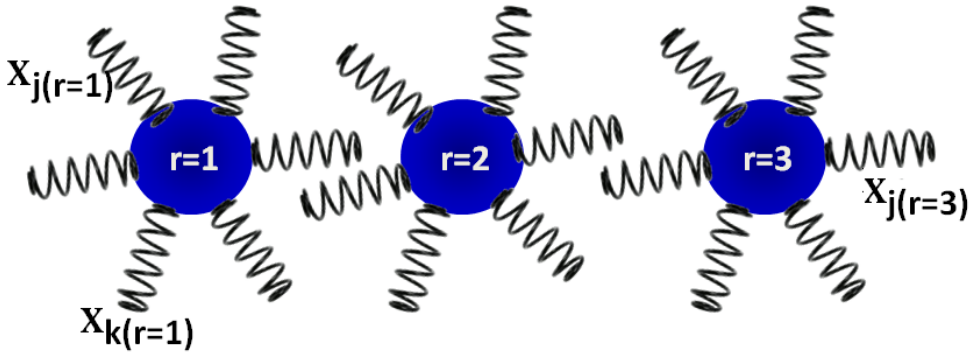

Figure 1: Graphic representation of how the reservoir is coupled to the electromagnetic field. At each position (r=1, r=2...) the electromagnetic field is coupled with an infinite set of harmonic oscillators. The bath oscillators, X_j, are pictured as springs, each of them characterized by its frequency, j, and its position.

$$L_{total} = \frac{\varepsilon_0}{2}\int d^3r(\mathbf{E}^2(\mathbf{r},t) - c^2\mathbf{B}^2(\mathbf{r},t)) \; + \sum_j \int dr^3(\; \frac{1}{2}\mu\dot{\mathbf{x}}_\mathbf{j}^\mathbf{2}(\mathbf{r},t) - \frac{1}{2}\mu\omega_j^2\mathbf{x}_\mathbf{j}^\mathbf{2}(\mathbf{r},t)) + \\ - \sum_j \alpha_j \int d^3r(\dot{\mathbf{x}}_\mathbf{j}(\mathbf{r},t)\mathbf{A}(\mathbf{r},t) + U(\mathbf{r},t)\nabla\cdot\mathbf{x}_\mathbf{j}(\mathbf{r},t)), \tag{14}$$

where ω_j and μ stand for the resonator frequency and mass respectively. Each mode of the reservoir is coupled to the electromagnetic field with a different coupling constant α_j, being j the oscillator's frequency [15].

Notice that Eq.(14) is a Lagrangian and, therefore, it can be quantized. If Eq.(14), when the bath degrees of freedom are integrated out, produces the macroscopic Maxwell equations for absorbing media, then we will have confirmed that this model reproduces the actual behaviour. This is what we show below.

For simplifying the calculation, it is desirable to work on the reciprocal space. For example, the electric field is written as (to distinguish the fields in real and reciprocal space, we shall underline the latter):

$$\mathbf{E}(\mathbf{r},t) = \frac{1}{(2\pi)^{3/2}}\int d^3k\underline{\mathbf{E}}(\mathbf{k},t)e^{i\mathbf{kr}}, \tag{15}$$

It is convenient to express the Lagrangian in terms of the vector and scalar potentials ($\underline{\mathbf{A}}$ and $\underline{U}$) in the Couloumb Gauge $\mathbf{k}\cdot\underline{\mathbf{A}} = 0$ in which $\underline{\mathbf{A}}$ is purely transversal [16].

The Lagrangian can be split in a parallel part, where the bath modes do not couple with the electromagnetic field and will be ignored [See appendix B], and a transverse part given by

$$L_{total}^{\perp} = \varepsilon_0 \int' d^3k(|\dot{\underline{\mathbf{A}}}| - c^2k^2|\underline{\mathbf{A}}|^2) + \sum_j \int' dk^3(\mu|\dot{\underline{\mathbf{x}}}_\mathbf{j}^\perp|^2 - \mu\omega_j^2|\underline{\mathbf{x}}_\mathbf{j}^\perp|^2) \\ - \sum_j \alpha_j \int' dk^3\; (\dot{\underline{\mathbf{x}}}_\mathbf{j}^\perp\cdot\underline{\mathbf{A}}^* + \dot{\underline{\mathbf{x}}}_\mathbf{j}^{*\perp}\cdot\underline{\mathbf{A}}). \tag{16}$$

Here the prime means that the integration is restricted to half of the reciprocal space.

For now on we will work with the Lagrangian density $\mathcal{L}$ to avoid writing all the integrals.

3.2 Classical Equations of Motion: Langevin Equation

Our goal is to find the motion equation of $\underline{A}$ and check if our model describes a lossy media with a Lagrangian formalism in the same way that the Maxwell's equations do (Eq.(9)).

We introduce the unit polarization vectors $\mathbf{e}^\lambda(\mathbf{k})$, $\lambda = 1, 2$, which are orthogonal to $\mathbf{k}$ and between them, and decompose the transverse fields along them to get:

$$\underline{\mathbf{A}}(\mathbf{k}, t) = \sum_{\lambda=1,2} \underline{A}^\lambda(\mathbf{k}, t)\mathbf{e}^\lambda(\mathbf{k}). \tag{17}$$

Now we are ready to write the Euler-Lagrange equations for $x_j^{*\lambda\perp}$ and $A^{\lambda *}$. Taking into account that they are continuous fields, their motion equations read as [16]

$$\partial_t \frac{\partial L}{\partial \underline{\dot{x}}_j^{\lambda *}} = \frac{\partial L}{\partial \underline{x}_j^{\lambda *}} - \sum_i \partial_i \frac{\partial L}{\partial(\partial_i \underline{x}_j^{\lambda *})} \tag{18}$$

$$\partial_t \frac{\partial L}{\partial \underline{\dot{A}}^{\lambda *}} = \frac{\partial L}{\partial \underline{A}^{\lambda *}} - \sum_i \partial_i \frac{\partial L}{\partial(\partial_i \underline{A}^{\lambda *})}, \tag{19}$$

where $\partial_i = \dfrac{\partial}{\partial k_i}$.

Omitting the fields' polarization, the equations to solve are

$$\boxed{\mu \underline{\ddot{x}}_j + \mu\omega_j^2 \underline{x}_j = \alpha_j \underline{\dot{A}}} \tag{20}$$

and

$$\boxed{\varepsilon_0 \underline{\ddot{A}} = -\varepsilon_0 c^2 k^2 \underline{A} - \sum_j \alpha_j \underline{\dot{x}}_j} \tag{21}$$

Since we want a motion equation for the EM field, we formally solve Eq.(20), which is nothing but a driven harmonic oscillator, and after, we insert the solution for $\underline{\dot{x}}_j$ in Eq.(21). The motion equations for the vector potential in the Fourier space of $\mathbf{k}$ and ω [See Appendix C] turn out to be

$$-\int_{-\infty}^{\infty} d\omega\omega^2 \varepsilon_0 A(\mathbf{k}, \omega) e^{-i\omega t} = -\int_{-\infty}^{\infty} d\omega \varepsilon_0 c k^2 A(\mathbf{k}, \omega) e^{-i\omega t} - \sum_j \alpha_j \dot{x}_j^h(\mathbf{k}, t) \ + \int_{-\infty}^{\infty} d\omega\omega^2 A(\mathbf{k}, \omega)\lambda(\omega). \tag{22}$$

Here, x_j^h is the solution of the homogeneous equation $\mu \underline{\ddot{x}}_j + \mu\omega_j^2 \underline{x}_j = 0$ and

$$\lambda(\omega) = P[\int \frac{J(\omega')}{\omega' - \omega} d\omega'] + i\frac{\pi}{2} J(\omega), \tag{23}$$

where $J(\omega)$ is defined as

$$J(\omega) = \sum_j \frac{\alpha_j^2}{\mu\omega_j} \delta(\omega - \omega_j). \tag{24}$$

If we set

$$\varepsilon(\omega) = \varepsilon_0 + \lambda(\omega), \tag{25}$$

we finally get the classical Langevin equation

$$-\int_{-\infty}^{\infty} d\omega\omega^2\varepsilon(\omega)A(\mathbf{k},\omega)e^{-i\omega t} = -\int_{-\infty}^{\infty} d\omega\varepsilon_0 c^2k^2A(\mathbf{k},\omega)e^{-i\omega t} - \sum_j \alpha_j\dot{x}_j^h(\mathbf{k},t). \tag{26}$$

In order to compare the equation of motion derived from this model, and the macroscopic Maxwell equation in a absorbing media, Eq.(9) , we shall write Eq.(26) in terms of the electric field. With that in mind, we use that $E = -\frac{\partial}{\partial t}\mathbf{A}(\mathbf{k},t) = i\omega\mathbf{A}(\mathbf{k},\omega)$, carry out the Fourier transform of $\sum_j \alpha_j\dot{x}_j^h(\mathbf{k},t)$ and remove the integrals to arrive at

$$-\frac{\omega^2}{c^2}\bar{\varepsilon}(\omega)E(\mathbf{k},\omega) + k^2E(\mathbf{k},\omega) = i\omega\mu_0\frac{i\omega\sum_j \alpha_j x_j^h(\mathbf{k},\omega)}{\mu_0c^2\varepsilon_0}, \tag{27}$$

where we have defined $\bar{\varepsilon}(\omega) = \dfrac{\varepsilon(\omega)}{\varepsilon_0} = \bar{\varepsilon_R}(\omega) + i\bar{\varepsilon_I}(\omega)$.

Eq.(27) is a Langevin equation and it is equivalent to the macroscopic classical equation in a dielectric derived from Maxwell's equations [See Eq.(9)] with a phenomenological current.

The term $\varepsilon(\omega)$, which has been first introduced in Eq.(25) and comes from modelling the dissipation as a bath of oscillators, corresponds with the dielectric permittivity. Its real and imaginary parts are related to each other through the Kramers-Kronig relations (cf. Eqs. (23) and (25)):

$$\bar{\varepsilon_R}(\omega) - 1 = \frac{\mathcal{P}}{\pi}\int d\omega' \frac{\bar{\varepsilon_I}(\omega)}{\omega' - \omega} \tag{28}$$

$$\bar{\varepsilon_I}(\omega) = -\frac{\mathcal{P}}{\pi}\int d\omega' \frac{\bar{\varepsilon_R}(\omega) - 1}{\omega' - \omega} \tag{29}$$

as the permittivity of real dielectric does [17].

3.3 Quantization

Once we have checked that our model accounts for the macroscopic Maxwell equations in dielectric, we quantize it. Given the Lagrangian density

$$\mathcal{L}_{total}^{\perp} = \varepsilon_0|\underline{\dot{\mathbf{A}}}| - \varepsilon_0c^2k^2|\underline{\mathbf{A}}|^2 + \sum_j(\mu|\underline{\dot{\mathbf{x}}}_\mathbf{j}^{\perp}|^2 - \mu\omega_j^2|\underline{\mathbf{x}}_\mathbf{j}^{\perp}|^2) - \sum_j \alpha_j(\underline{\dot{\mathbf{x}}}_\mathbf{j}^{\perp}\underline{\mathbf{A}^*} + \underline{\dot{\mathbf{x}}}_\mathbf{j}^{*\perp}\cdot\underline{\mathbf{A}}) \tag{30}$$

The generalized momentum read

$$\underline{\Pi} = \frac{\partial\mathcal{L}}{\partial\underline{\dot{A}^*}} = \varepsilon_0\underline{\dot{A}} \tag{31}$$

$$\underline{\Pi}^* = \frac{\partial\mathcal{L}}{\partial\underline{\dot{A}}} = \varepsilon_0\underline{\dot{A}}^* \tag{32}$$

$$\underline{P_j} = \frac{\partial\mathcal{L}}{\partial\underline{\dot{x}}_j^*} = \mu\underline{\dot{x}}_j - \alpha_j\underline{A} \tag{33}$$

$$\underline{P_j}^* = \frac{\partial\mathcal{L}}{\partial\underline{\dot{x}}_j} = \mu\underline{\dot{x}}_j^* - \alpha_j\underline{A}^*. \tag{34}$$

The canonical quantization imposes that a variable and its associated momentum follow a com-

mutation relation between them. Said commutation reads, for instead, for $\underline{\hat{A}}$ as

$$[\underline{\hat{A}}(\mathbf{k}), \underline{\hat{\Pi}}(\mathbf{k}')] = 0 \tag{35}$$

$$[\underline{\hat{A}}(\mathbf{k}), \underline{\hat{\Pi}}^*(\mathbf{k}')] = i\hbar\delta(\mathbf{k}' - \mathbf{k}), \tag{36}$$

yielding to the Hamiltonian density,

$$\mathcal{H} = \frac{1}{\varepsilon_0}|\underline{\hat{\Pi}}|^2 + \varepsilon_0 c^2 k^2 |\underline{\hat{A}}|^2 + \sum_j \left(\frac{1}{\mu}|\underline{\hat{P}}_j + \alpha_j \underline{\hat{A}}|^2 + \mu\omega_j^2 |\underline{\hat{x}}_j|^2 \right). \tag{37}$$

We recall that the underlined variables depend on $\mathbf{k}$ and t.

We are now in conditions to find the quantum version of Maxwell equations (Eqs.(9) or (27)) applying twice the Heisenberg equations to $\underline{\hat{x}}_j$, as $\dot{\underline{\hat{x}}}_j = \frac{i}{\hbar}[\hat{H}, \underline{\hat{x}}_j]$, and to $\underline{\hat{A}}$, as $\dot{\hat{A}} = \frac{i}{\hbar}[\hat{H}, \underline{\hat{A}}]$. In this way, we end up with the same motion equation showed in Eqs. (20) and (21), but quantized

$$\mu\ddot{\underline{\hat{x}}}_j + \mu\omega_j^2 \underline{\hat{x}}_j = \alpha_j \dot{\underline{\hat{A}}} \tag{38}$$

and

$$\varepsilon_0 \dot{\underline{\hat{A}}} = -\varepsilon_0 c k^2 \underline{\hat{A}} - \sum_j \alpha_j \dot{\underline{\hat{x}}}_j. \tag{39}$$

Therefore their solution is the quantum version of Eq.(26). It reads as

$$-\int_{-\infty}^{\infty} d\omega \omega^2 \varepsilon(\omega) \hat{A}(\mathbf{k}, \omega) e^{-i\omega t} = -\int_{-\infty}^{\infty} d\omega \varepsilon_0 c k^2 \hat{A}(\mathbf{k}, \omega) e^{-i\omega t} - \sum_j \alpha_j \underline{\hat{x}}_j^h(\mathbf{k}, t). \tag{40}$$

Our final step is to deal with the last term: write $\underline{\hat{x}}_j^h$ in terms of the creation and annihilation operators which increase (or decrease) an excitation of the bath field. This description comes naturally because $\underline{\hat{x}}_j^h$ follows the motion equation of a harmonic oscillator

$$\mu\ddot{\underline{\hat{x}}}_j + \mu\omega_j^2 \underline{\hat{x}}_j = 0, \tag{41}$$

with Lagrangian given by

$$\hat{\mathcal{L}}_j = \mu|\dot{\underline{\hat{x}}}_j|^2 + \mu\omega_j^2 |\underline{\hat{x}}_j|^2 = 0. \tag{42}$$

Here, the position variable is $\underline{\hat{x}}_j$ and its momentum $\underline{\hat{p}}_j = \dfrac{\partial \hat{\mathcal{L}}_j}{\partial \dot{\underline{\hat{x}}}_j^*} = \mu\dot{\underline{\hat{x}}}_j$.

Therefore $\dot{\underline{\hat{x}}}_j$ in terms of the position and its momentum is

$$\dot{\underline{\hat{x}}}_j^h = -\omega_j \underline{\hat{x}}_j(0) sin(\omega_j t) + \underbrace{\dot{\underline{\hat{x}}}_j(0)}_{\frac{\underline{\hat{P}}_j(0)}{\mu}} cos(\omega_j t) \tag{43}$$

with ω_j positive.

Introducing the creation and annihilation operators

$$\hat{f}_j = \sqrt{\frac{\mu\omega_j}{2\hbar}}(\hat{x}_j + \frac{i}{\mu\omega}\hat{P}_j) \tag{44}$$

$$\hat{f}_j^\dagger = \sqrt{\frac{\mu\omega_j}{2\hbar}}(\hat{x}_j - \frac{i}{\mu\omega}\hat{P}_j), \tag{45}$$

Eq.(43) can be rewritten as

$$\hat{\dot{x}}_j^h(\mathbf{k},t) = i\sqrt{\frac{\hbar\omega_j}{2\mu}}(\hat{f}_j^\dagger e^{i\omega_j t} - \hat{f}_j e^{-i\omega_j t}). \tag{46}$$

The equation above is included in Eq.(40). However, since our goal is to determinate the behaviour of each $\hat{A}(\mathbf{k},\omega)$, we transform the summation in modes j into an integral in ω [See Appendix D], yielding to

$$\sum_j \alpha_j \hat{\dot{x}}_j^h(\mathbf{k},t) = \int_0^\infty d\omega\sqrt{J(\omega)}\sqrt{\mu\omega}\; i\sqrt{\frac{\hbar\omega}{2\mu}}(\hat{f}_\omega^\dagger e^{i\omega t} - \hat{f}_\omega e^{-i\omega t}). \tag{47}$$

Notice that the integral goes from zero to ∞ because of the definition of $\hat{\dot{x}}_j^h$.

$J(\omega)$ is related to the permittivity's imaginary part. From Eqs. (23) and (25) it is determined that

$$\sqrt{J(\omega)} = \sqrt{\frac{2}{\pi}\varepsilon_I(\omega)}. \tag{48}$$

Putting all together Eqs. (40), (47) and (48) we write:

$$-\int_{-\infty}^{\infty} d\omega\omega^2\varepsilon(\omega)\hat{A}(\mathbf{k},\omega)e^{-i\omega t} = -\int_{-\infty}^{\infty} d\omega\varepsilon_0 ck^2\hat{A}(\mathbf{k},\omega)e^{-i\omega t} -$$
$$+\sqrt{\frac{\hbar}{\pi}}\int_0^\infty d\omega\;\sqrt{\varepsilon_I}\;(-i\;\omega\hat{f}_\omega^\dagger e^{i\omega t} + i\;\omega\hat{f}_\omega e^{-i\omega t}). \tag{49}$$

Due to $\hat{A}(\mathbf{r},t)$ is an hermitian operator, we can split the integrals in positive and negative ω as $\int_{-\infty}^{\infty} d\omega\hat{A}(\mathbf{k},\omega) = \int_0^\infty \hat{A}^+(\mathbf{k},\omega) + \int_0^\infty \hat{A}^-(\mathbf{k},\omega)$. We get

$$-\int_0^\infty d\omega\omega^2(\varepsilon(\omega)\hat{A}^+(\mathbf{k},\omega)e^{-i\omega t} + \varepsilon(-\omega)\hat{A}^-(\mathbf{k},\omega)e^{i\omega t}) =$$
$$-\int_0^\infty d\omega\varepsilon_0 ck^2(\hat{A}^+(\mathbf{k},\omega)e^{-i\omega t} + \hat{A}^-(\mathbf{k},\omega)e^{i\omega t}) + \sqrt{\frac{\hbar}{\pi}}\int_0^\infty d\omega\;\sqrt{\varepsilon_I}\;(-i\;\omega\hat{f}_\omega^\dagger e^{i\omega t} + i\;\omega\hat{f}_\omega e^{-i\omega t}). \tag{50}$$

Here, the imaginary unit that goes with the operators $\hat{f}_\omega^\dagger$ and $\hat{f}_\omega$ is arbitrary. It comes from the way in which these operators have been defined and from the initial phase we chose for the expression of $\hat{f}_\omega^\dagger$ and $\hat{f}_\omega$. Moreover, if we include the change $\hat{f}_\omega \to i\hat{f}_\omega$ and $\hat{f}_\omega^\dagger \to -i\hat{f}_\omega^\dagger$, the commutation relations are the same and Eq.(50) for positive ω reads

$$-\varepsilon(\omega)\omega^2 A^+(\mathbf{k},\omega) = -\varepsilon_0 c^2k^2A^+(\mathbf{k},\omega) + \sqrt{\frac{\hbar}{\pi}}\sqrt{\varepsilon_I}\;\omega\hat{f}_\omega, \tag{51}$$

with an equivalent expression for the negative part.

Eq.(51) can be expressed in terms of the transversal electric field. Being $\hat{E}^\perp(\mathbf{k},t) = -\dfrac{\partial}{\partial t}\hat{A}(\mathbf{k},t)$

, then $\hat{E}(\omega) = -i\omega\hat{A}(\omega)$. In this way, the equation is transformed to

$$-\varepsilon(\omega)\omega^2\hat{E}^+(\mathbf{k},\omega) = -\varepsilon_0 c^2 k^2 \hat{E}^+(\mathbf{k},\omega) + i\omega\sqrt{\frac{\hbar}{\pi}}\sqrt{\varepsilon_I}\,\omega\hat{f}_\omega. \tag{52}$$

Defining $\bar{\varepsilon}(\mathbf{k},\omega) = \dfrac{\varepsilon(\mathbf{k},\omega)}{\varepsilon_0}$ and given the equivalence $\mu_0\varepsilon_0 = \dfrac{1}{c^2}$ we obtain:

$$k^2\hat{E}^+(\mathbf{k},\omega) - \bar{\varepsilon}(\omega)\frac{\omega^2}{c^2}\hat{E}^+(\mathbf{k},\omega) = i\omega\mu_0(\omega\sqrt{\frac{\hbar\varepsilon_0}{\pi}}\sqrt{\bar{\varepsilon_I}}\hat{f}_\omega(\mathbf{k},\omega)). \tag{53}$$

The equation for the total transversal field is found by adding the hermitian conjugated.

$$\boxed{k^2\hat{E}(\mathbf{k},\omega) - \bar{\varepsilon}(\omega)\frac{\omega^2}{c^2}\hat{E}(\mathbf{k},\omega) = i\omega\mu_0\omega\sqrt{\frac{\hbar\varepsilon_0}{\pi}}\sqrt{\bar{\varepsilon_I}}(\hat{f}_\omega(\mathbf{k},\omega) - \hat{f}^\dagger_\omega(\mathbf{k},\omega))} \tag{54}$$

This is the "quantum version" of (27) and, thus, is the quantum macroscopic Maxwell equation. Notice that, opposite to the classical case, the noise current is never equal to zero because, even at $T = 0K$, $< f^2 >\neq 0$. That is, there are zero point fluctuations due to Heisenberg uncertainty. This is a remarkable difference with classical dynamics

3.4 Solutions

Maxwell's classical macroscopic equations in an absorbing, dispersive and homogeneous media in which the permittivity follows the Kramers-Kronig relation can be regarded as an operator field equations [18] which have the same appearance than Eq. (9):

$$k^2\hat{\mathbf{E}}(\mathbf{k},\omega) - \frac{\omega^2}{c^2}\bar{\varepsilon}(\omega)\hat{\mathbf{E}}(\mathbf{k},\omega) = i\omega\mu_0\hat{\mathbf{j}}(\mathbf{k},\omega). \tag{55}$$

with [cf. Eq.(54)]

$$\hat{\mathbf{j}}(\mathbf{k},\omega) = \omega\sqrt{\frac{\hbar\varepsilon_0}{\pi}}\sqrt{\bar{\varepsilon_I}(\omega)}(\hat{f}_\omega(\mathbf{k},\omega) - \hat{f}^\dagger_\omega(\mathbf{k},\omega)). \tag{56}$$

In real space Eq.(55) reads

$$\nabla\times\nabla\times\hat{\mathbf{E}}(\mathbf{r},\omega) - \frac{\omega^2}{c^2}\bar{\varepsilon}(\mathbf{r},\omega)\hat{\mathbf{E}}(\mathbf{r},\omega) = i\frac{\omega^2}{c^2}\sqrt{\frac{\hbar}{\pi\varepsilon_0}}\sqrt{\bar{\varepsilon_I}(\mathbf{r},\omega)}\,(\hat{f}_\omega(\mathbf{k},\omega) - \hat{f}^\dagger_\omega(\mathbf{k},\omega)). \tag{57}$$

The latter is an inhomogeneous differential equation where the solution is split as the sum of a homogeneous and a particular solution:

$$\hat{\mathbf{E}}(\mathbf{r},\omega) = \hat{\mathbf{E}}_{hom}(\mathbf{r},\omega) + \hat{\mathbf{E}}_{part}(\mathbf{r},\omega). \tag{58}$$

3.4.1 The Homogeneous Solution

We first find the solution for the homogeneous equation

$$k^2\hat{\mathbf{E}}_{hom}(\mathbf{k},t) + \frac{1}{c^2}\bar{\varepsilon}(\omega)\hat{\dot{\mathbf{E}}}_{hom}(\mathbf{k},t) = 0, \tag{59}$$

which is given by $\hat{\mathbf{E}}_{hom}(\mathbf{k},t) = \hat{\mathbf{E}}_{hom}(0,0)e^{it\left(\frac{ck}{\sqrt{\bar{\varepsilon}}}+\delta\right)}$. If $\bar{\varepsilon_i} \neq 0$, $\hat{\mathbf{E}}_{hom}$ tends to zero. Since we are not interested in transitory solutions, the only contribution comes from $\hat{\mathbf{E}}_{part}$. However, if there are not losses, the homogeneous solution does not decay and it reads [See Appendix A for a full derivation]

$$\hat{\mathbf{E}}_{hom}(\mathbf{r},t) = i\int d\omega \sqrt{\frac{\hbar\omega}{2\varepsilon_0}}(\hat{a}_\omega(t) - \hat{a}^\dagger_\omega(t))\mathbf{u}_\omega(\mathbf{r}). \tag{60}$$

Here, $\mathbf{u}_\omega(\mathbf{r})$ are the normalized spatial modes fulfilling the equation $\nabla\times\nabla\times\mathbf{v}(\mathbf{r}) + \bar{\varepsilon}\frac{\omega^2}{c^2}\mathbf{v}(\mathbf{r}) = 0$.

3.4.2 The Particular Solution: A Green's Function Approach

Making use of Green function formalism [See Appendix E for a review], the particular solution of Eq.(57) is

$$\boxed{\hat{\mathbf{E}}_{part}(\mathbf{r},\omega) = i\sqrt{\frac{\hbar}{\pi\varepsilon_0}}\,\frac{\omega^2}{c^2}\int d^3\mathbf{r}'\sqrt{\bar{\varepsilon_I}(\mathbf{r}',\omega)}\,\overleftrightarrow{G}(\mathbf{r},\mathbf{r}',\omega)(\hat{f}_\omega(\mathbf{r},\omega) - \hat{f}^\dagger_\omega(\mathbf{r},\omega))} \tag{61}$$

with $\overleftrightarrow{G}(\mathbf{r},\mathbf{r}',\omega)$ the Green dyadic function of the classical electric field

$$\left[\nabla\times\nabla\times - \frac{\omega^2}{c^2}\bar{\varepsilon}(\mathbf{r},\omega)\right]\overleftrightarrow{G}(\mathbf{r},\mathbf{r}',\omega) = \overleftrightarrow{I}\delta(\mathbf{r}-\mathbf{r}'). \tag{62}$$

A great accomplishment of this model is that the same Green function calculated for the classical electric field is used to find the quantum electric field. In addition, quantization can be done for arbitrary (and maybe phenomenological) permittivities [17].

If there are not absorption, $\varepsilon_I = 0$, the full solution is $\hat{\mathbf{E}} = \hat{\mathbf{E}}_{hom}$. However, if there are losses in the medium, $\hat{\mathbf{E}}_{hom} \to 0$, as we have argued in section 3.4.1. Thus, Eq.(61) is the full solution in this case.

The quantized electric field for a media without and with absorption, shown in Eq.(60) and (61), will be used in the next section to figure out how light and matter couple.

4 Light-Matter Interaction

When speaking of light-matter interaction, and specifically, the interaction between one emitter and the EM field, the geometry and electrical properties of the environment around the emitter play an important role. They can enhance or inhibit the coupling between them and lead to different behaviours. In this section, we will find how light and matter couple quantically and apply our results to different situations: the spontaneous emission, the physics of a cavity QED and a small emitter near a metallic surface. In the two later, light-matter interaction can show, under some conditions, different regimes: weak, strong and ultrastrong.

In order to describe the system behaviour, we start defining the Hamiltonian, which in general, can be split as

$$\hat{H}_{tot} = \hat{H}_{emitter} + \hat{H}_{rad} + \hat{H}_{int}. \tag{63}$$

The emitter can be an atom, a molecule or any particle small enough to apply the dipole approximation. Moreover, the emitter is considered to have only two energy levels. This kind of emitters are called two level system (TLS). Therefore, itis described by a two-dimensional state space formed by $|e\rangle$ and $|g\rangle$. The two states constitute a complete orthonormal system [2]. The emitter Hamiltonian is given by $\hat{H}_{emitter} = E_e |e\rangle \langle e| + E_g |g\rangle \langle g|$, and, if $E_e - E_g = \Delta$, it can be written as

$$\hat{H}_{emitter} = -\hbar \frac{\Delta}{2} \hat{\sigma}_z, \tag{64}$$

where $\hat{\sigma}_z$ is the Pauli matrix.

The radiation Hamiltonian [19],

$$\hat{H}_{rad} = \hbar \int d^3\mathbf{r} \int_0^\infty d\omega \; \omega \hat{f}^\dagger_\omega(\mathbf{r}, \omega) \hat{f}_\omega(\mathbf{r}, \omega), \tag{65}$$

is expressed in terms of the bath elementary excitation operators ($\hat{f}^\dagger_\omega$ and $\hat{f}_\omega$) which fulfil the bosonic commutation relations.

Let us focus now on $\hat{H}_{int}$. Starting from the minimal coupling Hamiltonian and applying the dipole approximation [15], the interaction Hamiltonian is written as

$$\hat{H}_{int} = -\hat{\mathbf{d}} \cdot \hat{\mathbf{E}}(\mathbf{r}_e, t), \tag{66}$$

where the electric field is evaluated at the position of the emitter. To figure out the above equation, we need the expression of the quantized electric field, which was previously found (Eq.61), and the electric dipole operator, $\hat{\mathbf{d}}$. We can express $\hat{\mathbf{d}} = q \cdot \hat{\mathbf{r}}$ in terms of the atom transition operators $\hat{\sigma}_{ij} = |i\rangle \langle j|$, where $|i\rangle$ and $|j\rangle$ can take the values $|g\rangle$ and $|e\rangle$ which stand for ground and excited states of the emitter, respectively. The electric dipole operator holds

$$\hat{\mathbf{d}} = \sum_{i,j} q \, |i\rangle \langle i| \, \hat{\mathbf{r}} \, |j\rangle \langle j| = \sum_{i,j} \mathcal{P}_{ij} \sigma_{ij}. \tag{67}$$

Here, $\mathcal{P}_{ij} = q \langle i| \hat{\mathbf{r}} |j\rangle$ is the electric dipole matrix element which, at least for an atomic emitter, the diagonal elements are equal to zero. That is because the atom eigenstates have a well defined parity [16] and, when the dipole momentum operator is applied, it changes it. Moreover, since $\hat{\mathbf{d}}$ is an operator, $\mathcal{P}_{ge} = \mathcal{P}_{eg} = \mathbf{d}$.

The total quantum Hamiltonian is given by

$$\hat{H}_{total} = -\hbar \frac{\Delta}{2} \hat{\sigma}_z + \hbar \int d^3\mathbf{r} \int_0^\infty d\omega \; \omega \hat{f}^\dagger_\omega(\mathbf{r}, \omega) \hat{f}_\omega(\mathbf{r}, \omega) - \hat{\sigma}_x \mathbf{d} \cdot \hat{\mathbf{E}}(\mathbf{r}_e). \tag{68}$$

with $\hat{\mathbf{E}}(\vec{r}_e) = \int_0^\infty \mathrm{d}\omega \hat{\mathbf{E}}(\mathbf{r}_e, \omega)$.

Here we consider the case of an absorbing media, while expressions for a non-absorbing media can be found in Appendix F. Using Eqs.(61) and (68) we get

$$\boxed{H_{int} = -\hat{\sigma}_x \int_0^\infty \mathrm{d}\omega \int \mathrm{d}^3\mathbf{r}' g(\omega, \mathbf{r}', \mathbf{r}_e) \left(\hat{f}(\mathbf{r}', \omega) - \hat{f}^\dagger(\mathbf{r}', \omega) \right)} \tag{69}$$

This is an important equation since the interaction Hamiltonian represents the coupling between

TLS and EM field. Here, we have introduced the shorthand notation

$$g(\omega, \mathbf{r}', \mathbf{r}_e) = i\sqrt{\frac{\hbar}{\pi\varepsilon_0}}\frac{\omega^2}{c^2}\sqrt{\bar{\varepsilon}_i(\mathbf{r}', \omega)}\,\mathbf{d}\overleftrightarrow{G}(\mathbf{r}_e, \mathbf{r}', \omega)\,, \tag{70}$$

being $\mathbf{r}_e$ the emitter position.

To understand qualitatively what the coupling to the field produces in the emitter, we split $\sigma_x = \sigma_+ + \sigma_-$ with

$$\hat{\sigma}_+ = |e\rangle\langle g| \tag{71}$$

$$\hat{\sigma}_- = |g\rangle\langle e|\,. \tag{72}$$

Thus, σ_+ takes a TLS in the ground into the excited state, whereas σ_- takes a TLS in the excited state into the ground state.

Moreover, we define the *collective modes* $\hat{b}(\omega)$ [15],

$$\int \mathrm{d}^3\mathbf{r}'\, g(\omega, \mathbf{r}', r_e) f(\mathbf{r}', \omega) \equiv \hbar g(\omega)\hat{b}(\omega), \tag{73}$$

which fulfil the bosonic commutation relation

$$[\hat{b}(\omega), \hat{b}^\dagger(\omega')] = \delta(\omega - \omega') \tag{74}$$

and lead to

$$|g(\omega)|^2 = \frac{1}{\pi\varepsilon_0\hbar}\frac{\omega^4}{c^4}\int \mathrm{d}^3r'\,\bar{\varepsilon}_i(\mathbf{r}', \omega)\vec{d}^T\overleftrightarrow{G}(\mathbf{r}_e, \mathbf{r}', \omega)\,\overleftrightarrow{G}^*(\mathbf{r}_e, \mathbf{r}', \omega)\vec{d}. \tag{75}$$

The interaction Hamiltonian expressed in terms of the new notation is

$$\hat{H}_{int}^{absorption} = -\hbar(\hat{\sigma}_+ + \hat{\sigma}_-)\int d\omega\; g(\omega)\left(\hat{b}(\omega) - \hat{b}(\omega)^\dagger\right). \tag{76}$$

Finally, by using the relation for the Green's tensor [18]

$$\frac{\omega^2}{c^2}\int \mathrm{d}^3\mathbf{r}'\,\bar{\varepsilon}_i(\mathbf{r}', \omega)\overleftrightarrow{G}(\mathbf{r}_e, \mathbf{r}', \omega)\,\overleftrightarrow{G}^*(\mathbf{r}_e, \mathbf{r}', \omega) = \mathrm{I}m[\overleftrightarrow{G}(\mathbf{r}_e, \mathbf{r}_e, \omega)] \tag{77}$$

we end up with

$$\boxed{|g(\omega)|^2 = \frac{1}{\hbar\pi\varepsilon_0}\frac{\omega^2}{c^2}\vec{d}^T\mathrm{I}m[\overleftrightarrow{G}(\mathbf{r}_e, \mathbf{r}_e, \omega)]\vec{d}} \tag{78}$$

$|g(\omega)|^2$ has units of $\omega(rad/s)$ and characterizes the coupling between one electromagnetic mode and the emitter. As it is shown in Appendix F, it coincides with the non-absorbing case ($\bar{\varepsilon}_i = 0$). Notice that the coupling depends on the imaginary part of Green's function and, in turn, on the emitter's environment. The modulus square of the coupling constant $|g(\omega)|^2$, called spectral density, characterizes the coupling between the system and the EM field.

4.1 Spontaneous Emission

Spontaneous emission is the process in which a quantum mechanical system transits from an excited energy state to a lower energy state, emitting a quantum in the form of a photon [2]. We

study the spontaneous emission when the temperature is equal to the absolute zero. In this case, the decay is produced by the point zero oscillations of the field modes.

In our formalism, spontaneous emission occurs when the initial state of the electromagnetic field is $|00...00\rangle$ (no photons), and the atom is in the excited state. Each number in $|00...00\rangle$ gives the number of EM excitations with a given energy. We are able to work with a state with no photons because we are at $0K$. Since the field and the emitter are described in different Hilbert spaces, the initial wave function of the total system is the tensor product $|e\rangle \otimes |00.....0\rangle$. These states, which describe at the same time light and matter, are called dressed states [20].

In order to find the spontaneous emission rate, γ, we take advantage of Fermi's golden rule which evaluates the probability of finding the system in the upper state $|g\rangle$ starting from $|e\rangle$ as

$$P_{e\to g} = \frac{1}{\hbar^2}\left|\int_0^t \langle g|\, \hat{H}^I_{int}(t)\, |e\rangle\, dt\right|^2 . \tag{79}$$

Here, the exponent I stands for interaction picture. The emission rate, γ, is found as the derivative in time of this probability.

The interaction Hamiltonian shown in Eq.(76) has four terms. The term $\hat{a}(\omega)^\dagger\sigma_-$ describes the process in which the emitter pass from the upper to the lower state and a photon of energy ω is emitted. The term $\hat{a}(\omega)\sigma_+$ describes the opposite process. The number of excitations is conserved in both of the processes [2]. On the other hand, the term $\hat{a}(\omega)\sigma_-$ describes the situation in which a photon is annihilated and the TLS falls from $|e\rangle$ to $|g\rangle$, resulting in the loss of approximately $2\hbar\omega$. Similarly $\hat{a}^\dagger\sigma_+$ results in the gain of $2\hbar\omega$. When Fermi's golden rule is applied in first order approximation, as we are doing, the coupling constant, $g(\omega)$, must be much smaller than the energy gap between the eigenstate of the unperturbed Hamiltonian. In our case this gap is equal to Δ. If that condition is fulfilled, the terms $\hat{a}^\dagger\sigma_+$ and $\hat{a}(\omega)\sigma_-$ can be neglected [2]. This is called the rotational wave approximation (RWA).

The probability of the system to fall from the excited to the ground state emitting a photon is found evaluating Eq.(79)[1]

$$P_{e\to g} = 2\pi t\, |g(\omega)|^2\, \delta(\omega - \Delta). \tag{80}$$

Deriving with respect to time, the spontaneous transition per unit time reads

$$\gamma = 2\pi\, |g(\omega)|^2\, \delta(\omega - \Delta)\ . \tag{81}$$

We can calculate the intrinsic lifetime of a quantum emitter which is equivalent to the spontaneous emission rate in vacuum as $2\pi|g(\omega)|^2$. Knowing that the imaginary part of Green function in vacuum is $\frac{1}{6\pi}\frac{\omega}{c}$ [21], we obtain

$$\boxed{\gamma_0 = \frac{|\vec{d}|^2\Delta^3}{3\pi\varepsilon_0\hbar c^3}} \quad \left(\frac{1}{s}\right) \tag{82}$$

which in terms of the fine structure constant, and being $\vec{d} = e\vec{r}$, reads

$$\gamma_0 = \frac{4}{3}\alpha\frac{r^2\Delta^3}{c^2} \quad \left(\frac{1}{s}\right). \tag{83}$$

4.2 Cavity QED

A cavity QED is an electromagnetic resonator with an atom inside. It can be built with two spherical mirrors with ultra high reflectivity facing each other placed millimetres apart [22]. [See Fig.6]. The behaviour of the EM field within the cavity is similar to a guitar string. In this simile, the mirrors would act as the holdings of the string and the vibration of the string would be the EM field mode[1].

Perhaps, the most blow-minding aspect of cavities are their ability of harbour entangled states of light and matter [22]. That is, atoms and light field in a superposed state [4].

The cavity QED is tuned with a single atom transition. In other words, we study resonant or near resonant atom-cavity interactions where the energy difference between the two level of the TLS, $\hbar\Delta$, coincides with the energy of the mode tolerated by the cavity, $\hbar\Omega$. To keep it simpler, we first suppose that there are not dissipation.

Since only one mode is considered in a cavity QED we take the light-matter Hamiltonian, presented in Eq.(69), and select one mode. This leads to the quantum Rabi model:

$$\hat{H}_{Rabi} = \underbrace{-\hbar\frac{\Delta}{2}\hat{\sigma}_z + \hbar\Omega\hat{a}^\dagger\hat{a}}_{\hat{H}_0} - \hbar g\left(\hat{\sigma}_+ + \sigma_-\right)\left(\hat{a} - \hat{a}^\dagger\right) \tag{84}$$

Let us discuss the spectrum of (84), when g=0. In this case, the Rabi Hamiltonian is equal to $\hat{H}_0$. Therefore, being in resonance, $\Omega = \Delta$, the states with the same number of excitations have the same energy. For instance, the state $|g, N\rangle$ (TLS in the ground state and N photons in the cavity), is equivalent to $|e, N-1\rangle$ (TLS in the excited state and N-1 photons in the cavity).

When $g \neq 0$ but small, the degenerate levels split, having a gap energy proportional to g. This tells us that we can no longer think of the atom and photon as separate entities [11].

We rewrite the interacting Hamiltonian of Eq.(84) as

$$\hat{H}_{int} = -\hbar g\left(\hat{\sigma}_+\hat{a} \ - \hat{\sigma}_-\hat{a}^\dagger \ - \hat{\sigma}_+\hat{a}^\dagger \ + \hat{\sigma}_-\hat{a}\ \right). \tag{85}$$

In first order of perturbation theory only $\hat{\sigma}_+\hat{a}$ and $\hat{\sigma}_-\hat{a}^\dagger$ play a role. The other terms, which involve mixing non-degenerate levels, are neglected. This is the RWA, already discussed in section 4.1. In doing so we obtain the, so called, Jaynes-Cumming Hamiltonian:

$$H_{JC} = -\hbar\frac{\Delta}{2}\hat{\sigma}_z + \hbar\Omega\hat{a}^\dagger\hat{a} - \hbar g\left(\hat{\sigma}_+\hat{a}\right) + h.c. \tag{86}$$

Jaynes-Cumming Hamiltonian conserves the number of excitations. We can compute the dynamic inside a subspace with a given number of excitations obtaining Rabi oscillations [20]:

$$|c_e(t)|^2 = cos^2(g\sqrt{n+1}t). \tag{87}$$

$|c^e(t)|^2$ is the probability for finding the atom in its excited state when working in a subspace with n+1 excitations. The frequency of the oscillations is proportional to the coupling constant and to

[1] These modes are the harmonics with $\omega = n\frac{\lambda}{2}$. Typically only one mode is considered: the one that is closer to the atomic transition.

the square root of the number of photons.

When the coupling, g, is increased, the perturbative argument breaks down and, as we can see in Fig. 2, the eigenvalues of the Rabi Hamiltonian split from the James-Cumming model eigenvalues. These effects are visible when the strength of the coupling, reaches a value around the tenth part of the field frequency, $0.1g \geq \Omega$. This regime is called he **ultrastrong regime.** The ultrastrong

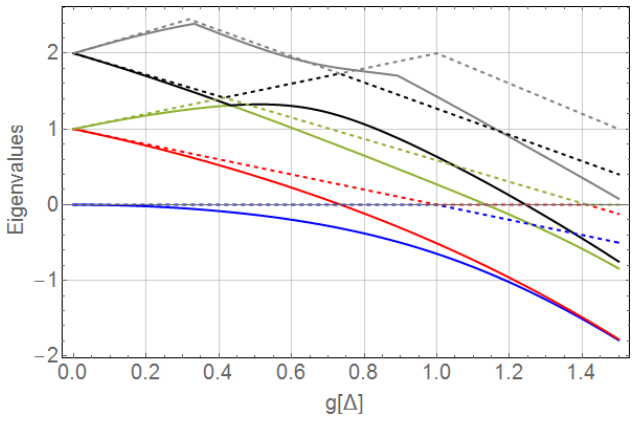

Figure 2: Energy splitting between the Rabi Hamiltonian eigenvalues and the Jaynes-Cumming eigenvalues.

coupling regime can be detected by measuring the emission spectra that it is asymmetric around the bare resonance frequency [23]. This regime may be interesting beyond fundamental research, it e.g. presents quantum nonlinear features at the single photon level [24]. Unfortunately, it is extremely difficult to achieve for traditional quantum optics systems such as atoms in cavities QED [6].

So far, we have not taken into account any kind of dissipation. However, in actual cavities QED there are two sources of dissipation: the spontaneous emission to different modes than the cavity mode, modelled by the decay rate γ; and the dissipation produced in the mirrors (leaks characterized by κ).

We will neglect the dissipation due to γ since we consider that the atom decays to other modes slower than how long takes the mode with frequency Δ to be dissipated by the mirrors. The mirror dissipation is modelled as a continuum bath of harmonic oscillators which couple with the EM field mode like Ohmic noise [25]. This bath model has been already discussed in section 2. The Hamiltonian of the atom, cavity and bath reads

$$\hat{H}_{Ohm} = -\hbar\frac{\Delta}{2}\hat{\sigma}_z + \hbar\Omega\hat{a}^\dagger\hat{a} - \hbar g\hat{\sigma}_x(\hat{a}-\hat{a}^\dagger) + \hbar\int d\omega\,\omega\hat{f}^\dagger\hat{f} + \hbar(\hat{a}^\dagger+\hat{a})\int d\omega\,\kappa(\omega)(\hat{f}_\omega+\hat{f}_\omega^\dagger), \quad (88)$$

where the three first terms accounts for the emitter, cavity mode and their coupling, whereas the two last are, in order of appearance, the Hamiltonian of a continuum set of harmonic oscillators (the bath), and its coupling with the cavity. The spectral density of the continuous bath modes, $\kappa(\omega)$, is assumed to be

$$J(\omega)_{Ohm} = \kappa^2(\omega) = \kappa\cdot\omega \;\; (eV)^2 \quad (89)$$

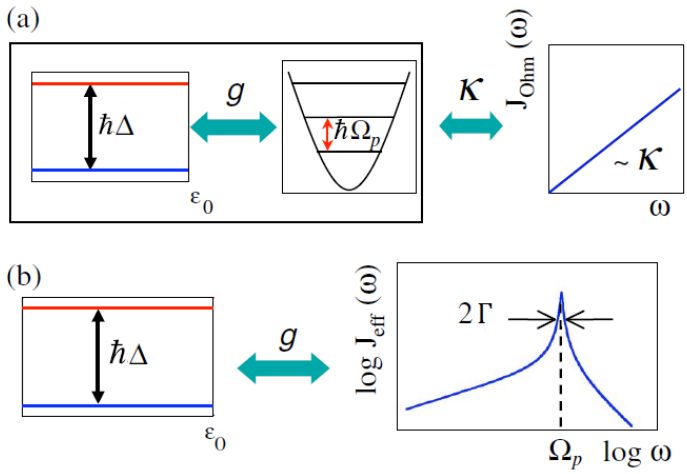

Figure 3: Schematic picture of the models used to describe a cavity QED with dissipation. In (a) the system is a TLS coupled to a harmonic oscillators (the EM field mode), which in turn is coupled to an Ohmic environment with spectral density $J_{Ohm}(\omega)$. In (b), the TLS is coupled to an environment with peaked spectral density $J_{eff}(\omega)$. Image taken from [25].

mimicking the effects of an Ohmic electromagnetic environment.

The model presented in Eq.(88) is equivalent to an atom coupled to a continuum, but with an effective spectral density, $J(\omega)$. This effective equivalent model is [25]

$$\hat{H}_{eff} = -\hbar\frac{\Delta}{2}\hat{\sigma}_z - \hbar g\hat{\sigma}_x \int d\omega g(\omega)(\hat{a} - \hat{a}^\dagger) + \hbar \int d\omega\, \omega \hat{a}^\dagger \hat{a}, \tag{90}$$

where the effective spectral density is a Lorentzian:

$$\boxed{g^2(\omega) = \frac{1}{\pi}\frac{g^2\Gamma/2}{(\Omega-\omega)^2 + \left(\frac{\Gamma}{2}\right)^2}} \tag{91}$$

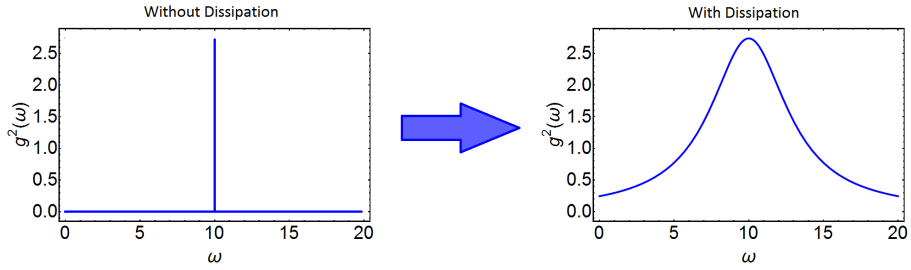

Figure 4: Spectral density of how the modes of the EM field couple with the emitter in a cavity QED. In the left without dissipation and in the right with dissipation.

If we compare the spectral density before and after including dissipation, we observe that, in the first case, the atom couples with only one EM mode, whereas when dissipation is included, the

spectral density is widened, inducing a decay in Rabi oscillations. [See Fig.(4)]

The challenge and goal, then, is to find the conditions in which the coupling strength between the atom and a particularly chosen single photonic mode is much stronger relative to all the others dissipative channels. In these conditions, we will be able to see Rabi oscillations decaying [See Fig.(5a)]. This regime is called **strong coupling** and it is characterized because the emitter and the EM field can exchange a photon several times before coherence is lost[8]. The strong coupling and, therefore, Rabi oscillations were first observed in 1987 (Brune *et al.*, 1987). The importance of strong regime resides in that, although difficult to achieve, is essential to produce relevant effects to quantum computation and cryptography [22].

When the spectral density shows a Lorentzian shape, the condition to observe Rabi oscillation is $g > \frac{1}{4}\Gamma$, and it can be calculated by Weisskoptf-Wigner theory [See Appendix G]. If that condition were not fulfilled, we would be in the **weak regime**, where there are not Rabi oscillations and the dynamic of the TLS population is regulated by a negative exponential [See Fig.(5b)].

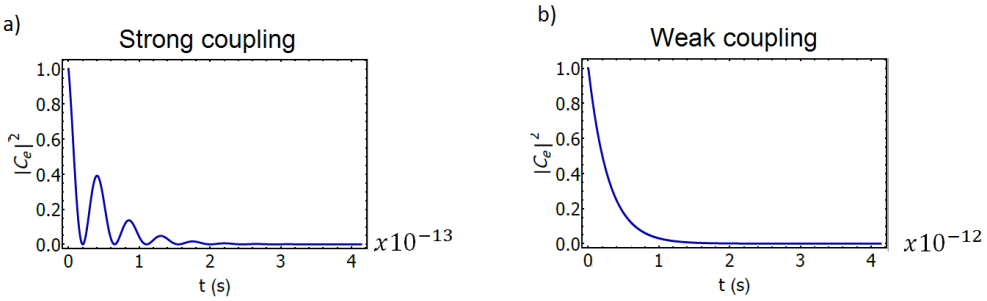

Figure 5: Probability of finding the emitter in the excited state among time. Figure 5 a) pictures the dynamic of the emitter in the strong regime, described by Rabi oscillations decaying with time and figure 5 b) in the weak regime described by an exponential decay.

5 A Small Emitter near Two-Dimensional Materials: Results and Discussion

In the interface between a metal, with $\varepsilon_r(\omega) << 0$, and a dielectric, with $\varepsilon_r(\omega) > 0$, the light interacts with the free electrons of the metal leading to electromagnetic waves bounded to the surface within the dielectric and charge motion within the metal surface [6]. These excitations of the EM field confined near the interface are called surface plasmon polaritons (SPPs).

SPPs loss energy while they propagate along the surface due to Ohmic losses which heat the metal. This dissipation is represented by the imaginary part of the metal permittivity. For this reason, metals with low $\varepsilon_i(\omega)$ like silver or gold are used in SPPs applications [15].

An emitter far from the interface decays radiating a photon like if it were in vacuum. When it is approached to a metallic surface (around 10-500 nm), the spectral density of the EM modes,

$|g(\omega)|^2$, is modified because of the existence of SSPs [26]. At that distance from the surface, the decay energy is transferred to a SPPs.

Besides SPPs, there are also other mechanisms through which the emitter can transfer its energy. If the distance between the TLS and the metal surface is smaller than, approximately, 10 nm, the energy of the decay is not used to create neither a photon nor an SPPs [See Fig.(7)]. In its place, that energy is transferred to the free electrons in the metal surface. The spectral density, $|g(\omega)|^2$, which is calculated using $Im[\overleftrightarrow{G}(\mathbf{r}_e, \mathbf{r_e}, \omega)]$, [See Eq.(78)], takes into account the EM modes coupled to the electronic current of the metal [26]. This current is extremely localized because it is dissipated very quickly by Joule effect, heating the metal.

We will study the behaviour of a TLS characterized by its intrinsic decay rate, γ_0, placed in the air (medium a) and near to a metallic surface made of silver or gold (medium m). The permittivities of the metals are defined via a fit to its real permittivity as:

$$\bar{\varepsilon}_m(\omega) = \bar{\epsilon}_{m,\infty} - \frac{\omega_p^2}{\omega(\omega + i\gamma_p)} - \delta_\varepsilon \frac{\omega_b^2}{\omega^2 - \omega_b^2 + i\omega\gamma_b}. \tag{92}$$

The first term corresponds to a Drude function describing a metal with only one band. Since metals band structure is more complicated, there are other contributions to the permittivity which can be written as a sum of functions with poles. The parameters utilized are showed in table 1 [27].

Metal	$\varepsilon_{m,\infty}$	ω_p	γ_p	δ_ε	ω_p	γ_b
Gold	5.967	8.729	0.065	1.09	2.684	0.433
silver	4.6	9.0	0.07	1.1	4.9	1.2

Table 1: Parameters needed to calculate electric permittivity of the metals gold and silver.

The macroscopic QED formalism for absorbing media developed in chapter 3 and 4 is perfectly appropriate for the description of this situation, since it characterizes the materials by their electric permittivity and takes into account the lossy character of the interaction. In this formalism, the emitter-plasmon Hamiltonian is shown in Eq.(76).

We can make an analogy between the atom in the nearby of a metallic surface and a cavity QED [See Fig.(6)]. Both of them are described by the same Hamiltonian and their only difference is the origin of the dissipation: while for a cavity QED is the photons that scape through the mirrors, the dissipation in the interface comes from ohmic losses associated with the metal [28].

We will analyse the properties of the emitter near to a metallic surface and its similarities with a cavity QED studying its spectral density. The magnitude that stands for the decay rate enhancement of the emitter when it is approached to the interface is the Purcell factor:

$$P(\mathbf{r}_e, \omega) = \frac{\gamma(\mathbf{r}_e, \omega)}{\gamma_0} = \frac{\vec{e}_d \, {}^T \mathrm{Im}[\overleftrightarrow{G}(\mathbf{r}_e, \mathbf{r}_e, \omega)]\vec{e}_d}{\mathrm{Im}[G(\omega)]_{\mathrm{vacuum}}}, \tag{93}$$

being $\gamma_0(\omega)$ the intrinsic decay rate, $\gamma(\mathbf{r}_e, \omega)$ the decay rate of an emitter at $\mathbf{r}_e$, $\vec{e}_d$ the emitter dipole moment unity vector and $\mathrm{Im}[G(\omega)]_{\mathrm{vacuum}} = \frac{1}{6\pi}\frac{\omega}{c}$. As we can see in Fig.(7), the Purcell factor can take values from up to 10^3

In the problem studied, we consider the interface between the air and the metal in the plane XY,

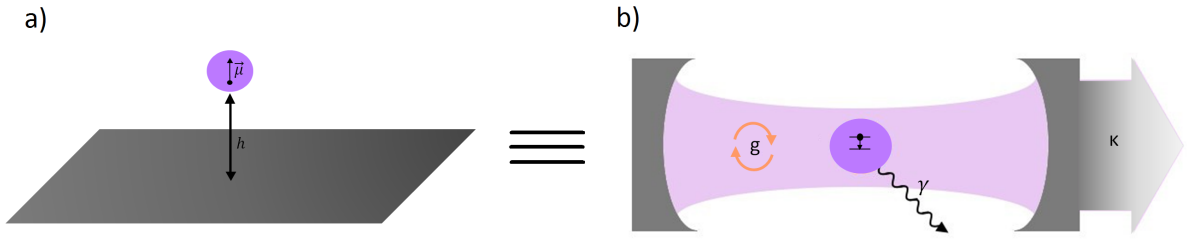

Figure 6: Comparison between an emitter near to a metallic surface and a Cavity QED.

with z=0 and the emitter placed in the air at (0,0,h) [See Fig.(6a)]. This layered structure produces a different Green dyadic above and below the interface which can be represented as follows:

$$\overleftrightarrow{G}(\mathbf{R},\omega) = \overleftrightarrow{G}_a(\mathbf{R},\omega) + \overleftrightarrow{G}_{Ram}(\mathbf{R},\omega) \qquad z>0 \tag{94}$$

$$\overleftrightarrow{G}(\mathbf{R},\omega) = \overleftrightarrow{G}_{Tam}(\mathbf{R},\omega) \qquad z<0, \tag{95}$$

being $\mathbf{R} = \mathbf{r}_e - \mathbf{r}'$, with $\mathbf{r}_e$ the emitter position and $\mathbf{r}'$ the position at which we are evaluating the Green function. The behaviour in the air is governed by the sum of the direct contribution of the emitter $\overleftrightarrow{G}_a$, which is the Green function of one emitter in vacuum, plus the reflected contribution $\overleftrightarrow{G}_{Ram}$. On the other hand, the behaviour in the medium m is regulated by the transmitted Green function, $\overleftrightarrow{G}_{Tam}$.

To calculate the spectral density in the dipole approximation we have to evaluate the Green dyadic produced by the emitter at the emitter position: $\mathbf{R} = 0$ and $z > 0$. We consider the emitter dipole momentum $\vec{d}$ transversally oriented to the surface because this is the most convenient direction to enhance the coupling [26]. Therefore, the terms of $Im[\overleftrightarrow{G}(\mathbf{r}_e,\mathbf{r}_e,\omega)]$ that we had to compute are reduced to $G_{zz}(\mathbf{0})$. Its explicit expression reads [21]

$$G_{zz}(\mathbf{0}) = \underbrace{\frac{ig}{4\pi}\int_0^\infty dq_{||}\frac{q_{||}^3}{q_{az}}}_{G_{zza}(\mathbf{0})} + \underbrace{\frac{-ig}{4\pi}\int_0^\infty dq_{||} r_{am}\frac{q_{||}^3}{q_{az}}e^{2iq_{az}\tilde{h}}}_{G_{zzRam}(\mathbf{0})} \qquad z>0 \tag{96}$$

Here, the wave vector and the emitter position are normalized as $|\tilde{h}| = g|h|$ and $q = \frac{|k|}{g}$, being $g = \frac{\omega}{c}$. In this way, $|q_a|^2 = \bar{\varepsilon}_a = 1$ in the air and $|q_m|^2 = \bar{\varepsilon}_m$ in the metal. Moreover, the wave vector is separated in its parallel part, $q_{||}$, and its transversal part, $q_z = \sqrt{\bar{\varepsilon} - q_{||}^2}$. r_{am} is the reflectivity and is written as

$$r_{am} = \frac{q_{mz} - q_{az}\bar{\varepsilon}_m}{q_{mz} + q_{az}\bar{\varepsilon}_m} \tag{97}$$

In order to find $G_{zzRam}(\mathbf{0})$ we need to solve the integral in Eq.(96). This is a bit tricky since the integrand includes poles in $\frac{1}{q_{az}}$ and in r_{am}. The later stands for the plasmons because it produces

a reflected wave even if there were no emitter. Moreover, the integrand includes branch cuts in q_{az} and q_{mz}. Hence, the integral was carried out in the complex plane avoiding the poles and the branch cuts [See Appendix H].

After evaluating $G_{zzRam}(\mathbf{0})$, the Purcell factor can be calculated from Eq.(93) as:

$$P(h,\omega) = 1 + \frac{G_{zzRam}(\mathbf{0})}{G_{zza}(\mathbf{0})}. \tag{98}$$

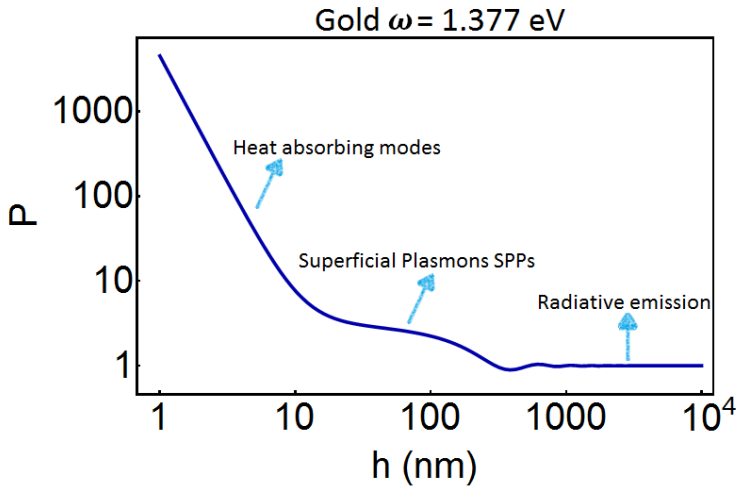

Figure 7: Purcell factor with respect to the distance when the emitter emission frequency is 1.377eV and the metallic surface is made of silver. The Purcell factor is modified when we approach the emitter to the surface. Far from the surface the TLS emits like if it were in vacuum. When is placed a few hundreds of nm apart from the surface the behaviour is governed by SPPs and very near to the surface the emission is dominated by extremely fast non-radiative lossy channels.

The spectral density, $|g(\omega)|^2$, can easily be calculated from the Purcell factor using Eq.(98) and (78). We compute this quantity for an emitter placed at different distance from the surface. Fig.(8) shows $2\pi|g(\omega)|^2$ for an emitter set at different distances from a gold and silver surface. We observed that, when the emitter is placed at 20nm or nearer from the surface, the spectral density has a Lorentzian shape, but if the emitter is moved away from the surface, we recover the spectral density of the vacuum. See Eq.(82).

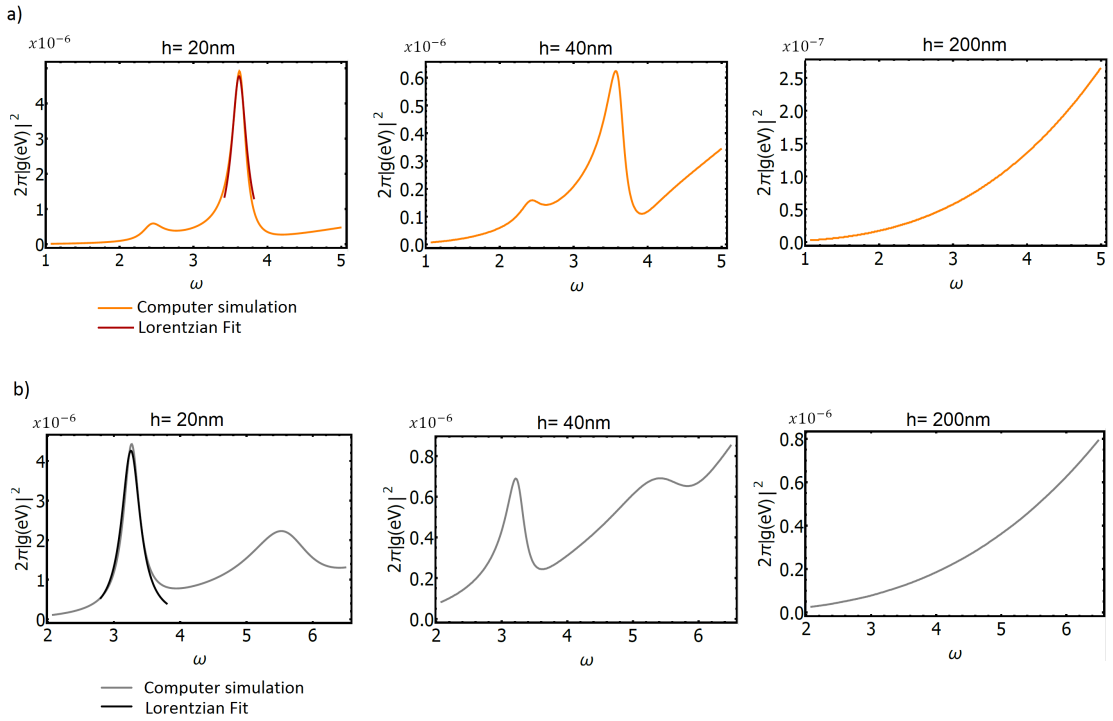

Figure 8: a) Photonic spectral density of an emitter near to a gold surface with respect to the frequency at different distances. b) The same but in a silver surface.

The effective Lorentzian found in the spectral density at distances smaller than 20nm from the surface does not come from the SPP contribution. It comes from the modes coupled to the electronic current which are more evanescent than SPPs [26]. If we observe the Purcell factor with respect to the distance in silver and gold evaluated at the frequency associated with the peak maximum (3.63eV for gold and 3.24eV for silver), we conclude that there are not SPPs contribution [see Fig.(9)]. Moreover, we will see that, to enter into the strong and ultrastrong regime, the emitter must be placed very close to the surface, where the dynamic is dominated by this non-radiative lossy channels.

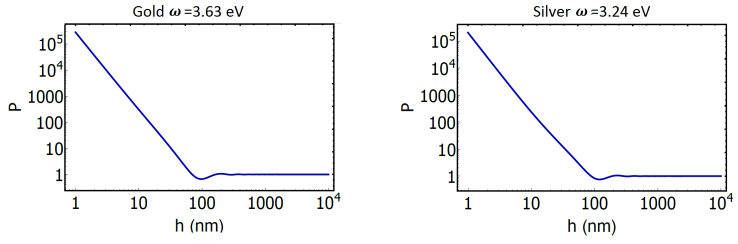

Figure 9: Purcell factor with respect to the distance of a TLS near to a gold metallic surface (left) and a silver metallic surface (right). The Purcell factor is evaluated at the frequency that corresponds with a maximum of the spectral density.

The Lorentzian shape of the spectral densities obtained [See Fig.(8)], confirms the equivalence between a cavity QED and an emitter near to a metallic surface [See section 4.2]. We fitted the obtained spectral densities to the Lorentzian of Eq.(91) in order to get the strength of the coupling, g, and its dissipation, Γ. What in the cavity was defined as the frequency of the EM mode harboured in the cavity, Ω, now is the frequency at the maximum of the effective Lorentzian.

Spectral density depends on both the intrinsic decay rate and the frequency. Its relation with the intrinsic decay rate, γ_0, is as follows

$$|g(\omega)|^2 = \gamma_0 \frac{6\pi c}{\omega} \, Im[G_{zz}(\mathbf{r}_e, \mathbf{r}_e, \omega)] \ . \tag{99}$$

The larger the intrinsic decay is, the stronger is the coupling. Moreover, comparing the above expression with Eq.(91) we can see that an increment in γ_0 enlarges g. So that, emitters with a big dipole moment helps to reach the strong and ultrastrong regime (recall that the conditions for strong and ultrastrong regime were $g > \frac{1}{4}\Gamma$ and $g > 0.1\Omega$, respectively).

In order to compute $|g(\omega)|^2$, we need to pick some values for γ_0. The chosen γ_0 coincide with the intrinsic decay rates of state-of-the-art emitters with large γ_0 such as nitrogen-vacancy centers, quantum dots or J aggregates [26]. Rabi oscillations predicted for an emitter close to a metallic surface have a period below $10^{-13}\left(\frac{1}{s}\right)$ [See Fig.(5)], these super-fast oscillations can be measured thanks to streak-camera experiments or interfermotric electron microscopy, since they have subpicosecond resolution [26].

We compare the necessary conditions for the strong regime when we are working with gold or silver in Fig.(10a). We observe that the conditions are pretty similar in both of the cases. That is because silver and gold have similar properties.

We can see in Fig.(10a) that, at least theoretically, strong coupling can be reached by an emitter near to a surface of gold or silver. This regime is favoured by large dipole momentum of the emitter and short distance between the TLS and the interface. We can not take into account the results for distances smaller than 1nm since our formalism relies on a macroscopic description of the materials and, at that distance, we can not describe the metal by its permittivity anymore. In agreement with our results, experimentally, there have been observations of the strong regime in ensembles of molecules near to one metallic surface [28].

We can also obtain the conditions in which the ultrastrong coupling is reached. Fig.(10b) certifies that it is possible to fulfil those conditions for distances larger than 1nm. In other words, this theory predicts ultrastrong regime within the limits of the performed approximations. Our results show that silver is more suitable to show ultrastrong regime than gold. This is because of, for silver, Ω is smaller and, in addition, g is slightly larger. Moreover, the same as in the strong regime, the ultrastrong regime is favoured by large intrinsic emission rates, γ_0, and short distances h.

In this work we have rediscovered the conditions to observe strong coupling regime of a emitter close to a metallic surface exposed in [26] and, in addition, we have theoretically proved that it is possible to arrive to the ultrastrong regime with a single atom emitter.

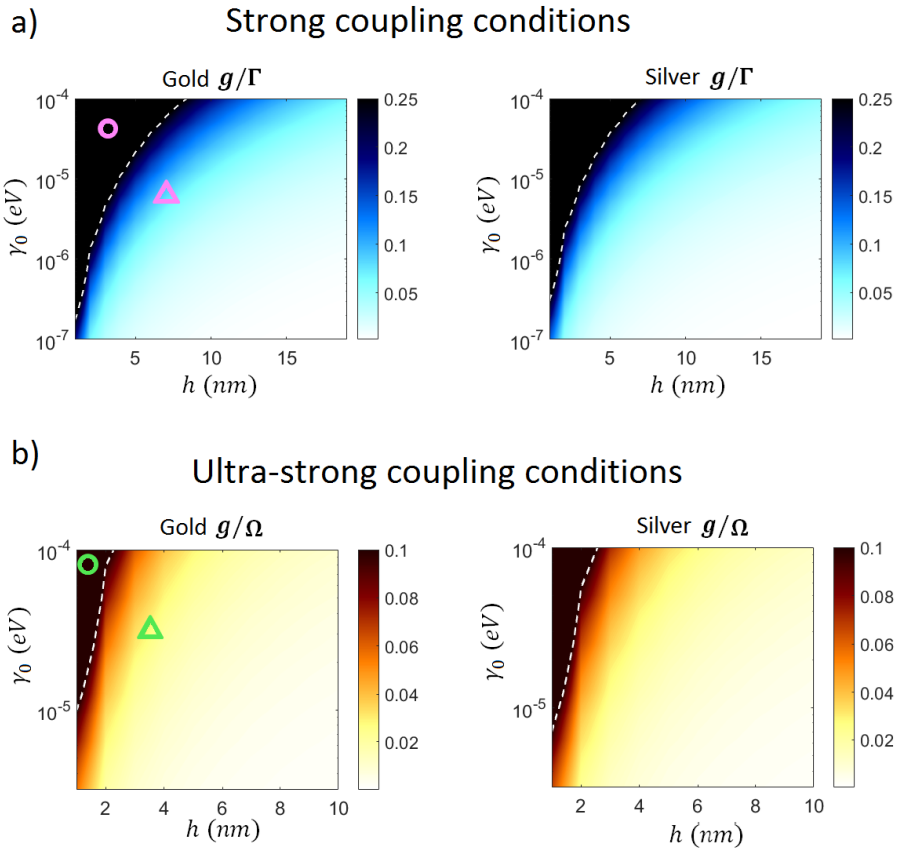

Figure 10: The figure 10a shows the ratio of the coupling, g, divided by the dissipation, Γ, with respect to the emitter intrinsic decay rate, γ_0, and the distance between emitter and surface, h. The white dashed line marks the border between weak and strong regime, $g/\Gamma = 1/4$. The zone marked with a circle corresponds to strong coupling and the zone marked with a triangle to weak coupling. On the other hand, figure 10b shows the ratio of the coupling, g, divided by the frequency associated with the maximum spectral density, Ω, with respect to the emitter intrinsic decay rate, γ_0, and the distance between emitter and surface, h. The white dashed line marks the border of the ultrastrong regime, $g/\Omega = 0.1$. Here the zone with a circle corresponds to the ultrastrong regime. The plots in the left shows the results found in a gold surface and the plots in the right in a silver surface.

6 Summary

In the present work we have revisited the quantization of the EM field in a dispersive and absorbing media where the dissipation is modelled via its interaction with a bath described as an infinite set of harmonic oscillators. The interaction of the field with this bath produces a quantum noisy current given by the linear momentum of the bath oscillators. This noisy current is never cancelled due to zero point fluctuations.

We observed that the quantized electric field in an absorbing media has the same spatial distribution than the classical field and, the same as classically, it can be calculated from the Green dyadic function.

We studied the interaction between a quantum emitter with two energy levels and the electric field in the dipole approximation. The function that represents how the emitter and the electric field are coupled depending on its frequency is called the *photonic spectral density*. It is represented by $|g(\omega)|^2$ and it contains all the information of the problem. $|g(\omega)|^2$ depends on the frequency of the EM mode, the intrinsic decay rate of the emitter and the surroundings of the emitter via the imaginary part of the Green function.

Over the present work we have shown three regimes of light-matter interaction (weak, strong and ultrastrong) through two examples: the vacuum and a cavity QED. In the weak regime, the exited atom emits a photon that is faded away in the surroundings. Hence, the dynamic is said to be irreversible. In the strong regime, light and matter are entangled. The spectral density has a peaked shape and, as a result, the atom couples stronger with one EM mode than with the others. The main feature of strong coupling is the apparition of Rabi oscillation in its dynamic. Finally, the ultrastrong regime is produced when the strength of the coupling is on the order of the emitter and the EM mode frequency.

Our research was focused on how the spectral density is modified when the emitter is placed in a dielectric and close to a metallic surface. We calculated the spectral density and the conditions required to achieve the strong and ultrastrong regime when the metallic surface was made of gold or silver.

7 Conclusions

The results show that an emitter made of a single atom with a plausible dipole moment can reach the strong regime when it is placed near to a metallic surface made of gold or silver. Opposite to what it could be thought, we have not achieved the strong coupling thanks to the SPPs, but thanks to the super-confined EM modes coupled to the electronic current of the metal (the Ohmic losses). The relevance of this result resides in that the strong regime is a challenge. Moreover, not only strong regime, but also ultrastrong regime was found. So far, ultrastrong regime was observed when the emitter was made of many atoms or circuits QED simulating an effective atom, both of them with huge dipole moments.

Although our calculations were made for a metallic surface of silver and gold, using the formalism developed, we could compute the spectral density and, consequently, the conditions to achieve the strong and ultrastrong regime for any material, if its electrical permittivity is known. In particular, the discovery of 2D materials with diverse properties opens a new door for further studies.

Other lines of research could be that, instead of studying the strong and ultrastrong coupling between an emitter and a field mode, we could see how two emitters exchange energy between them when they are coupled to one SPP or another localized modes.

References

[1] L. Novotny and B. Hecht, "Principles of nano-optics," (Cambridge university press, 2012) Chap. 8. Light emission and optical interactions in nanoscale environments, pp. 250–304.

[2] M. O. Scully and M. S. Zubairy, "Quantum optics," (AAPT, 1999) Chap. 6. Atom-field interaction:quantum theory, pp. 193–217.

[3] R. Eng, J. Butler, and K. Linden, Optical Engineering **19**, 945 (1980).

[4] S. Haroche, Rev. Mod. Phys. **85**, 1083 (2013).

[5] C. N. Cohen-Tannoudji, Reviews of Modern Physics **70**, 707 (1998).

[6] P. Törmä and W. L. Barnes, Rep. Prog. Phys. **78**, 013901 (2015).

[7] T. Schwartz, J. A. Hutchison, C. Genet, and T. W. Ebbesen, Physical review letters **106**, 196405 (2011).

[8] T. Niemczyk, F. Deppe, H. Huebl, E. Menzel, F. Hocke, M. Schwarz, J. Garcia-Ripoll, D. Zueco, T. Hümmer, E. Solano, *et al.*, Nature Physics **6**, 772 (2010).

[9] C. T. J. Alkemade, Applied Spectroscopy **35**, 1 (1981).

[10] J. A. Hutchison, T. Schwartz, C. Genet, E. Devaux, and T. W. Ebbesen, Angewandte Chemie International Edition **51**, 1592 (2012).

[11] H. J. Kimble, Nature **453**, 1023 (2008).

[12] A. Bolivar, Phys. Rev. A **58**, 4330 (1998).

[13] E. N. del Busto, "Caracterización de dieléctricos a frecuencia de microondas." (2004).

[14] B. Huttner and S. M. Barnett, Phys. Rev. A **46**, 4306 (1992).

[15] T. Hümmer, F. García-Vidal, L. Martín-Moreno, and D. Zueco, Phys. Rev. B **87**, 115419 (2013).

[16] C. Cohen-Tannoudji, *Atoms in electromagnetic fields*, Vol. 1 (World scientific, 1994).

[17] L. Knöll, S. Scheel, and D.-G. Welsch, *QED in dispersing and absorbing media*, Tech. Rep. (Theoretisch-Physikalisches Institut, 2000).

[18] H. T. Dung, L. Knöll, and D.-G. Welsch, Phys. Rev. A **57**, 3931 (1998).

[19] D. Dzsotjan, A. S. Sørensen, and M. Fleischhauer, Physical Review B **82**, 075427 (2010).

[20] T. M uller, "Quantum rabi oscillation a direct test of field quantization in a cavity," University of Mainz (2004).

[21] A. Nikitin, "Dyadic green's funtctions for diffraction problems." Universidad de Zaragoa (2012).

[22] N. D. Poulin, arXiv preprint (2014).

[23] X. Cao, J. Q. You, H. Zheng, and F. Nori, New Journal of Physics **13**, 073002 (2011).

[24] E. Sánchez-Burillo, J. García-Ripoll, L. Martín-Moreno, and D. Zueco, Faraday Discuss. **178**, 335 (2015).

[25] M. Goorden, M. Thorwart, and M. Grifoni, Physical review letters **93**, 267005 (2004).

[26] A. González-Tudela, P. Huidobro, L. Martín-Moreno, C. Tejedor, and F. García-Vidal, Phys. Rev. B **89**, 041402 (2014).

[27] P. B. Johnson and R.-W. Christy, Physical review B **6**, 4370 (1972).

[28] M. S. Tame, K. McEnery, Ş. Özdemir, J. Lee, S. Maier, and M. Kim, Nature Physics **9**, 329 (2013).

[29] W. P. Schleich, "Quantum optics in phase space," (Wiley-VCH Verlag GmbH & Co. KGaA, 2005) Chap. 10. Field Quantization, pp. 255–290.

[30] W. P. Schleich, H.-P. Breuer, and F. Petruccione, "The theory of open quantum systems," in *Quantum Master Equation* (Oxford University Press on Demand, 2002) Chap. 4. Quantum Master Equation, pp. 141–160.

[31] L. Martín-Moreno, "An introduction to green's functions in electromagnetism." Universidad de Zaragoa (2016).

A Quantization of the Electromagnetic Field in Vacuum

Electromagnetic field consists of discrete energy parcels, photons. Although the interaction between matter and light is normally introduced from a semi-classical point of view, this approach cannot describe a phenomena as known as spontaneous emission. In order to analyse, for instance, the behaviour in cavities QED, the Casimir effect and, in particular, emitters near to a two-dimensional material, a quantum formalism of the EM field is needed.

Almost all of the key results of quantizing the electromagnetic field can be derived by treating the electromagnetic field much like a harmonic oscillator. Indeed, we may be able to write the EM field as an infinite set of harmonic oscillators spatially distributed following the Classical Green's dyadic.

We start from Maxwell's equation in the SI units in vacuum:

$$\nabla \cdot \mathbf{B}(\mathbf{r},t) = 0 \tag{100}$$

$$\nabla \cdot \mathbf{D}(\mathbf{r},t) = \rho(\mathbf{r},t) \tag{101}$$

$$\nabla \times \mathbf{E}(\mathbf{r},t) = -\frac{\partial}{\partial t}\mathbf{B}(\mathbf{r},t) \tag{102}$$

$$\nabla \times \mathbf{H}(\mathbf{r},t) = \frac{\partial}{\partial t}\mathbf{D}(\mathbf{r},t) + \mathbf{j}(\mathbf{r},t). \tag{103}$$

Here ρ and $\mathbf{j}$ denote the charge and the current. The constitutive relations which relate the magnetic flux density $\mathbf{B}$ with the magnetic field $\mathbf{H}$ and the electric displacement $\mathbf{D}$ with the electric field $\mathbf{E}$ in non-magnetic materials are:

$$\mathbf{D} = \varepsilon\mathbf{E} \tag{104}$$

$$\mathbf{B} = \mu_0\mathbf{H}. \tag{105}$$

Introducing the vector and scalar potential, $\mathbf{A}$ and U respectively, using the Coulomb Gauge given by

$$\nabla \cdot \mathbf{A} = 0, \tag{106}$$

and assuming that we are in vacuum ($\rho = \mathbf{j} = 0$) the wave equation for the vector potential simplifies to [29]:

$$\nabla^2\mathbf{A} - \frac{\bar{\varepsilon}}{c^2}\frac{\partial^2}{\partial t^2}\mathbf{A} = 0. \tag{107}$$

We solve Eq.(107) proposing the ansatz

$$\mathbf{A}(\mathbf{r},t) = \Upsilon q(t)\mathbf{v}(\mathbf{r}). \tag{108}$$

That is, we use the method of variable separation. Here, $q(t)$ is a function dependent on time only and $\mathbf{v}(\mathbf{r})$ depends exclusively on position $\mathbf{r}$. Υ is a constant. Replacing this ansatz in Eq.(107) and being (j=x,y,z) we find

$$\frac{\nabla^2 v_j(\mathbf{r})}{v_j(\mathbf{r})} = \frac{\bar{\varepsilon}}{c^2}\frac{\ddot{q}(t)}{q(t)}. \tag{109}$$

Because both sides are independent from $\mathbf{r}$ or t, they are equal to constants. The left-hand side contains a second derivative with respect to position, thus, the constant has units of $|(length)^{-2}|$. We call it $-|\vec{k}|^2 = k^2$, where $\vec{k}$ is the wave vector determined by the spatial boundary condition.

We obtain, in this way, the Helmholth equation,

$$\nabla^2\mathbf{v}(\mathbf{r}) + k^2\mathbf{v}(\mathbf{r}) = 0, \tag{110}$$

for the spatial part of the vector potential and an oscillator like equation,

$$\ddot{q}(t) + \omega^2 q(t) = 0, \tag{111}$$

for the time dependent part. Here, $\omega \equiv \frac{c}{\sqrt{\bar{\varepsilon}}}|\vec{k}|$ is the wave length determined by the boundary conditions applied in the spatial part. For example, the tangential component of $\mathbf{E}$ and the normal component of $\mathbf{B}$ vanish in the borders when the field is considered within a cavity of metal walls. These conditions of the electromagnetic field in the cavity lead to several discrete possible solutions called modes. Each solution k_l is associated to a mode $\mathbf{v}(\mathbf{r})$. The mode functions $\mathbf{u}_l(\mathbf{r})$ are $\mathbf{v}_l(\mathbf{r})$ normalised, $\int d^3r \mathbf{u_l}(\mathbf{r})\mathbf{u_{l'}}(\mathbf{r}) = \delta_{l,l'}$.

The mode functions $\mathbf{u}_l(\mathbf{r})$ determine the spatial dependence of the vector potential $\mathbf{A}$, and can be proven to be orthonormal and complete for a cavity of rather arbitrary shape [29]. Therefore, we expand $\mathbf{A}$ into the mode functions as

$$\mathbf{A}(\mathbf{r},t) = \sum_l q_l(t)\mathbf{u}_l(\mathbf{r}), \tag{112}$$

where, so far, any condition restricts the mode amplitudes $q_l(t)$. Eq.(112) yields the corresponding electric and magnetic mode expansion:

$$\mathbf{E}(\mathbf{r},t) = -\frac{\partial \mathbf{A}}{\partial t} = -\sum_l \dot{q}_l(t)\mathbf{u}_l(\mathbf{r}) \tag{113}$$

$$\mathbf{H}(\mathbf{r},t) = \frac{1}{\mu_0}\nabla \times \mathbf{A} = \sum_l q_l(t)\nabla \times \mathbf{u}_l(\mathbf{r}) \tag{114}$$

If we take the spatial part and we go backwards using again the equation $\nabla \times (\nabla \times \mathbf{A}) = \nabla(\nabla \cdot \mathbf{A}) - \nabla^2\mathbf{A}$ we can rewrite Eq.(110) as

$$\nabla \times \nabla \times \mathbf{v}(\mathbf{r}) + \bar{\varepsilon}\frac{\omega^2}{c^2}\mathbf{v}(\mathbf{r}) = 0. \tag{115}$$

This expression is worth keeping to compare with the results shown in the next sections. It could be noticed that, so far, all the development is purely classical.

A.1 The Field as a Set of Harmonic Oscillators

Starting from the Lagrangian of the electromagnetic field in vacuum,

$$L = \varepsilon_0 \int d^3r \left[\frac{1}{2}\mathbf{E}^2(\mathbf{r},t) - c^2\frac{1}{2}\mathbf{B}^2(\mathbf{r},t)\right], \tag{116}$$

we derive its associated Hamiltonian because, in order to quantize, we need a Hamiltonian framework.

$$H \equiv \int d^3r \left[\frac{1}{2}\varepsilon_0\mathbf{E}^2(\mathbf{r},t) + \frac{1}{2}\mu_0\mathbf{B}^2(\mathbf{r},t)\right]. \tag{117}$$

The integration extends over all the space and we do not assume a specific form of the resonator.

Replacing Eqs.(113) and (114) in the Hamiltonian expressed in Eq.(117) and carrying out the integration over the space we arrive at [See Ref[29] for details]:

$$H = \sum_l H_l = \sum_l \left[\frac{1}{2}\dot{q}_l^2 + \frac{1}{2}\omega_l^2 q_l^2\right]. \tag{118}$$

Once the EM field has been written as a sum of harmonic oscillators, the quantization program is trivial following the steps learnt for a classical oscillator.

A.2 Quantization of the Electromagnetic Field

The quantization is carried out postulating the commutation relation

$$[\hat{q}_l, \hat{p}_l] = i\hbar\delta_{l,l'}. \tag{119}$$

We introduce the creation and annihilation operators, which in our case add or remove photons from a system,

$$\hat{a}_l \equiv \frac{1}{\sqrt{2\hbar\omega_l}}(\omega_l \hat{q}_l + i\hat{p}_l) \tag{120}$$

$$\hat{a}_l^\dagger \equiv \frac{1}{\sqrt{2\hbar\omega_l}}(\omega_l \hat{q}_l - i\hat{p}_l). \tag{121}$$

It is easy to check that, from the canonical relations [Eq.(119)], we obtain the well known result for the creation and annihilation operators:

$$[\hat{a}_l, \hat{a}_l^\dagger] = \delta_{l,l'}. \tag{122}$$

Finally, the Hamiltonian for the EM field reads

$$\hat{H} = \sum_l \frac{1}{2}\hbar\omega_l(\hat{a}_l^\dagger \hat{a}_l + \hat{a}_l \hat{a}_l^\dagger) = \sum_l \hbar\omega_l(\hat{a}_l^\dagger \hat{a}_l + \frac{1}{2}), \tag{123}$$

where the second term of the Hamiltonian is a consequence of the commutation relation and describes a sum over all the zero-point energies of the individual mode oscillators.

The final goal of this appendix was to find the quantified electric field. Using Eq.(113) and $\hat{\dot{q}}(t) = p(t)$ we end up with

$$\hat{\mathbf{E}}(\mathbf{r}, t) = \sum_l i\sqrt{\frac{\hbar\omega_l}{2\varepsilon_0}} \left(\hat{a}_l(t) - \hat{a}_l^\dagger(t)\right) \mathbf{u}_l(\mathbf{r}). \tag{124}$$

Notice that $\hat{\mathbf{E}}$ is an operator, and the time dependence indicates that we are working in the Heisenberg picture. Therefore, if we explicitly write their time dependence

$$\boxed{\hat{\mathbf{E}}(\mathbf{r}, t) = \sum_l i\sqrt{\frac{\hbar\omega_l}{2\varepsilon_0}} \left(\hat{a}_l e^{-i\omega_l t} - \hat{a}_l^\dagger e^{i\omega_l t}\right) \mathbf{u}_l(\mathbf{r})} \tag{125}$$

Eq.(125) is a crucial result. On one hand, "mathematically", it says that the quantized EM field has quantum time dependent fluctuations given by the creation and annihilation operators ($a_l(t)$ and $a_l^\dagger(t)$). On the other hand, "physically", Eq.(125) tells us what a photon is: an excitation of the EM field. Its spatial profile is given by $\mathbf{u}_l(\mathbf{r})$.

A.3 The Continuous Form of the Quantized Electromagnetic Field

So far we have expressed the quantized electric field as a sum of modes as in Eq.(125). However, it is possible to express it as an integral in frequencies.

We firstly convert the sum in modes l using the rectangle rule $\sum_l \delta_l = \int dl$. However, we have to take into account how the operators $\hat{a}_l$ and the modes $\mathbf{u}_l$ varies.

The commutation rules between the operators creation of Eq.(122) and annihilation should remain invariant

$$[\hat{a}_l, \hat{a}_{l'}^\dagger] = \frac{\delta_{l,l'}}{\delta_l} \xrightarrow{\delta_k \to 0} \delta(l - l'). \tag{126}$$

In this way, the discrete operator $\hat{a}_l$ is transformed to the operator $\dfrac{\hat{a}_l}{\sqrt{\delta_l}}$ in the continuum.

The mode $\mathbf{u}_l$ is defined to be orthonormal. They fulfil the equation

$$\int d^3r\, \mathbf{u}_l^* \mathbf{u}_{l'} = \delta_{l,l'}. \tag{127}$$

When going to the continuum these modes changes in the same way as the operators creation and annihilation:

$$\mathbf{u}_l \longrightarrow \frac{\mathbf{u}_l}{\sqrt{\delta_l}}. \tag{128}$$

The electric field expressed as a integral of modes is given by

$$\hat{\mathbf{E}}(\mathbf{r},t) = i\int dl\ \sqrt{\frac{\hbar\omega_l}{2\varepsilon_0}}(\hat{a}_l(t) - \hat{a}_l^\dagger e^{i\omega_l t})(t)\mathbf{u}_l(\mathbf{r}). \tag{129}$$

We only have left the change of variable from l to ω. Performing it, the Dirac function transforms as

$$\int d\omega\ \delta(\omega-\omega') = \int dl\ \frac{d\omega}{dl}\delta(\omega-\omega') \longrightarrow \delta(l-l') = \frac{d\omega}{dl}\delta(\omega-\omega'). \tag{130}$$

Using the same invariant conditions as before, the creation and annihilation operators are modified to

$$\hat{a}_l \longrightarrow \hat{a}_\omega\sqrt{\frac{d\omega}{d_l}} \tag{131}$$

and the modes to

$$\mathbf{u}_l \longrightarrow \mathbf{u}_\omega\sqrt{\frac{d\omega}{d_l}} \tag{132}$$

Carrying out the variable change $dl = d\omega\cdot\frac{dl}{d\omega}$, the electric field finishes as

$$\hat{\mathbf{E}}(\mathbf{r},t) = i\int d\omega\ \sqrt{\frac{\hbar\omega}{2\varepsilon_0}}(\hat{a}_\omega(t) - \hat{a}_\omega^\dagger(t))\mathbf{u}_\omega(\mathbf{r}). \tag{133}$$

The energy of the Electromagnetic field can also be transformed to

$$\hat{H} = \int d\omega\hbar\omega(\hat{a}_\omega^\dagger\hat{a}_\omega + \frac{1}{2}), \tag{134}$$

B Derivation of the Lagrangian of the EM Field, the Bath and their Interaction

In this appendix we start from

$$L_{total} = L_{EM} + L_{Bath} + L_{int} \tag{135}$$

$$L_{total} = \frac{\varepsilon_0}{2}\int d^3r(\mathbf{E}^2(\mathbf{r},t) - c^2\mathbf{B}^2(\mathbf{r},t))\ +\ \sum_j\int dr^3(\ \frac{1}{2}\mu\dot{\mathbf{x}}_\mathbf{j}^\mathbf{2}(\mathbf{r},t) - \frac{1}{2}\mu\omega_j^2\mathbf{x}_\mathbf{j}^\mathbf{2}(\mathbf{r},t)) +$$
$$-\sum_j\alpha_j\int d^3r(\dot{\mathbf{x}}_\mathbf{j}(\mathbf{r},t)\mathbf{A}(\mathbf{r},t) + U(\mathbf{r},t)\nabla\cdot\mathbf{x}_\mathbf{j}(\mathbf{r},t)), \tag{136}$$

and we want to arrive at an equation of the Lagrangian easier to handle.

For the calculation, it is convenient to work on the reciprocal space. For example, the electric field is written as

$$\mathbf{E}(\mathbf{r},t) = \frac{1}{(2\pi)^{3/2}}\int d^3k\underline{\mathbf{E}}(\mathbf{k},t)e^{i\mathbf{kr}}, \tag{137}$$

where, to differentiate between the fields in real and reciprocal space, we shall underline the latter.

In the reciprocal space, the Lagrangian in Eq.(136) reads

$$L_{EM} = \varepsilon_0\int' d^3k(|\underline{\mathbf{E}}|^2 - c^2|\underline{\mathbf{B}}|^2) \tag{138}$$

$$L_{bath} = \sum_j \int' d^3k(\mu|\underline{\dot{\mathbf{x}}_\mathbf{j}}|^2+\mu\omega^2|\underline{\mathbf{x}_\mathbf{j}}|^2). \tag{139}$$

$$L_{int} = -\sum_j \alpha_j \int' d^3k(\underline{\dot{\mathbf{x}}_\mathbf{j}}\,\underline{\mathbf{A}^*} + i\mathbf{k}\underline{U}^*\underline{\mathbf{x}_\mathbf{j}} + \underline{\dot{\mathbf{x}}_\mathbf{j}^*}\,\underline{\mathbf{A}} - i\mathbf{k}\underline{U}\underline{\mathbf{x}_\mathbf{j}^*})). \tag{140}$$

Here, the prime means that the integration is restricted to half of the reciprocal space.

From our previous experience with the quantization in vacuum, we shall use the Couloumb gauge and express the Lagrangian in terms of the vector and scalar potentials $\underline{\mathbf{A}}$ y $\underline{U}$.

The relation between the potentials and the fields in the Fourier space are

$$\underline{\mathbf{B}}(\mathbf{k}) = i\mathbf{k}\times\underline{\mathbf{A}} \tag{141}$$

$$\underline{\mathbf{E}} = -\partial_t\underline{\mathbf{A}} - i\mathbf{k}\underline{U}. \tag{142}$$

The Coulomb's Gauge in the Fourier space is given by ($\mathbf{k}\cdot\underline{\mathbf{A}} = 0$). Notice that $\mathbf{A}$ is purely transversal in this Gauge. This fact facilitates the actual calculations. In fact, the magnetic field is also transversal, whereas the electric field has a transversal part which comes from $\underline{\mathbf{A}}$, and a parallel one from $\underline{U}$.

Putting all together, the Lagrangian relative to the EM field reads

$$L_{EM} = \varepsilon_0 \int' d^3k(|\underline{\dot{\mathbf{A}}}|^2+k^2|\underline{U}|^2-c^2k^2|\underline{\mathbf{A}}|^2). \tag{143}$$

We observe that $\underline{\dot{U}}$ does not appear in the total Lagrangian. Therefore $\underline{U}$ is not, formally speaking, a dynamic variable of the motion. $\underline{U}$ can be eliminated of the Lagrangian using the Euler-Lagrange equations for $\underline{\dot{U}^*}$. In this way we obtain

$$\underline{U}(\mathbf{k},t) = \frac{i}{\varepsilon_0 k}\sum_j \alpha_j \underline{\mathbf{x}_\mathbf{j}}^{||} \tag{144}$$

The final total Lagrangian is:

$$L_{total} = L_{EM} + L_{bath} + L_{int} \tag{145}$$

$$L_{EM} = \varepsilon_0 \int' d^3k(|\underline{\dot{\mathbf{A}}}|^2+\frac{1}{\varepsilon_0^2}|\sum_j \alpha_j \underline{\mathbf{x}_\mathbf{j}}^{||}|^2-c^2k^2|\underline{\mathbf{A}}|^2) \tag{146}$$

$$L_{bath} = \sum_j \int' dk^3(\mu|\underline{\dot{\mathbf{x}}_\mathbf{j}}|^2-\mu\omega_j^2|\underline{\mathbf{x}_\mathbf{j}}|^2) \tag{147}$$

$$L_{int} = -\int' dk^3\,(\frac{2}{\varepsilon_0}|\sum_j \alpha_j \underline{\mathbf{x}_\mathbf{j}}^{||}|^2+\sum_j \alpha_j \underline{\dot{\mathbf{x}}_\mathbf{j}}\cdot\underline{\mathbf{A}^*}+\sum_j \alpha_j \underline{\dot{\mathbf{x}}_\mathbf{j}^*}\cdot\underline{\mathbf{A}}) \tag{148}$$

This can be split in a parallel trivial part, for which the parallel bath does not coupled with the EM field ($\underline{\mathbf{A}}$ is purely transversal), and a transverse part:

$$L_{total}^{\perp} = \varepsilon_0 \int' d^3k(|\underline{\dot{\mathbf{A}}}|-c^2k^2|\underline{\mathbf{A}}|^2) + \sum_j \int' dk^3(\mu|\underline{\dot{\mathbf{x}}_\mathbf{j}}^{\perp}|^2-\mu\omega_j^2|\underline{\mathbf{x}_\mathbf{j}}^{\perp}|^2)$$
$$-\sum_j \alpha_j \int' dk^3\,(\underline{\dot{\mathbf{x}}_\mathbf{j}}^{\perp}\cdot\underline{\mathbf{A}}^* + \underline{\dot{\mathbf{x}}_\mathbf{j}}^{*\perp}\cdot\underline{\mathbf{A}}). \tag{149}$$

This equation is easier to handle in order to obtain the motion equation by the Euler-Lagrange equation applied in the variables $\underline{\mathbf{A}}$ and $\underline{U}$

C The Classical Motion Equations of Huttner and Barnett's Model

Along this Appendix we will solve the equations

$$\boxed{\mu\ddot{\underline{x}}_j + \mu\omega_j^2\underline{x}_j = \alpha_j\dot{\underline{A}}} \tag{150}$$

and

$$\boxed{\varepsilon_0\ddot{\underline{A}} = -\varepsilon_0 c^2k^2\underline{A} - \sum_j \alpha_j\dot{\underline{x}}_j} \tag{151}$$

Eq.(150) is the equation of a harmonic oscillator driven by an external time dependent "force": $\alpha_j\dot{\underline{A}}$. Its general solution is

$$\underline{x}_j = \underline{x}_j^h + \frac{\alpha_j}{\mu\omega_j}\int_{t_0}^{t} dt' sin(\omega_j(t-t'))\dot{\underline{A}}(t'), \tag{152}$$

being the homogeneous solution,

$$\underline{x}_j^h = \underline{x}_j(0)cos(\omega_j t) + \frac{\dot{\underline{x}}_j}{\omega_j}sin(\omega_j t). \tag{153}$$

Our goal is to solve this motion equation to check if our model describes a lossy media with a Lagrangian formalism in the same way that the Maxwell's equation do (Eq.(9)). With this propose, we first perform an integration by parts over the integral of (152). Next, we derivative Eq.(152) with respect to time, t, using Liebniz integral rule to finally obtain $\dot{\underline{x}}_j$. After, we include the result of $\dot{\underline{x}}_j$ in Eq.(151) having

$$\varepsilon_0\ddot{\underline{A}} = -\varepsilon_0 c^2k^2\underline{A} - \sum_j \alpha_j\dot{\underline{x}}_j^h - \sum_j \frac{\alpha_j^2}{\mu\omega_j}\int_{t_0}^{t} sin(\omega_j(t-t'))\ddot{\underline{A}}(t')dt' \tag{154}$$

We focus in the integral $\int_{t_0}^{t} sin(\omega_j(t-t'))\ddot{\underline{A}}(t')dt'$ and we perform the variable change:

$$t - t' = \tau \;\longrightarrow\; \int_0^{t-t_0} d\tau. \tag{155}$$

Here, $t - t_0$ takes into account how long we go back in time. Since the reservoir is assumed to have a short memory, if we go backwards the integrand tends fast to zero. In this way, the limit of the integral $t - t_0$ can be extended to ∞. This is a usual procedure called Markovian approximation [30].

We also transform $\underline{A}$ to the Fourier space:

$$\underline{A}(\mathbf{k},t) = \int_{-\infty}^{\infty} A(\mathbf{k},\omega)e^{-i\omega t}d\omega \tag{156}$$

$$\ddot{\underline{A}}(\mathbf{k},t) = -\int_{-\infty}^{\infty} \omega^2 A(\mathbf{k},\omega)e^{-i\omega t}d\omega. \tag{157}$$

In this way, after all the approximations, the integral $\int_{t_0}^{t} sin(\omega_j(t-t'))$ changes to

$$\int_{-\infty}^{\infty} d\omega\omega^2\underline{A}(\mathbf{k},\omega)\underbrace{\sum_j \frac{\alpha_j^2}{\mu\omega_j}\int_0^{\infty} sin(\omega_j\tau)e^{-i\omega\tau}d\tau}_{\lambda(\omega)}. \tag{158}$$

where $\lambda(\omega)$ is defined as

$$\lambda(\omega) = \sum_j \frac{\alpha_j^2}{\mu\omega_j}\int_0^{\infty} sin(\omega_j\tau)e^{-i\omega\tau}d\tau. \tag{159}$$

We compute $\lambda(\omega)$

$$\lambda(\omega) = P[\int \frac{J(\omega')}{\omega' - \omega} d\omega'] + i\frac{\pi}{2} J(\omega), \tag{160}$$

defining

$$J(\omega) = \sum_j \frac{\alpha_j^2}{\mu\omega_j} \delta(\omega - \omega_j). \tag{161}$$

Finally, the motion equation for $\underline{A}(\mathbf{k}, \omega)$ (Eq.(154)) reads

$$-\int_{-\infty}^{\infty} d\omega \omega^2 \varepsilon_0 A(\mathbf{k}, \omega) e^{-i\omega t} = -\int_{-\infty}^{\infty} d\omega \varepsilon_0 c k^2 A(\mathbf{k}, \omega) e^{-i\omega t} - \sum_j \alpha_j \dot{x}_j^h(\mathbf{k}, t) \ + \int_{-\infty}^{\infty} d\omega \omega^2 A(\mathbf{k}, \omega) \lambda(\omega). \tag{162}$$

D From Discrete to Continuous Frequency

The road from discrete to continuum can be more tricky than it seems. In this appendix we transform the summation $\sum_j \alpha_j \dot{\hat{x}}_j^h$ to an integral.

$\dot{\hat{x}}_j^h(\mathbf{k}, t)$ depends on the operators $\hat{f}_j^\dagger$ and $\hat{f}_j^\dagger$ as

$$\dot{\hat{x}}_j^h(\mathbf{k}, t) = i\sqrt{\frac{\hbar\omega_j}{2\mu}} (\hat{f}_j^\dagger e^{i\omega_j t} - \hat{f}_j e^{-i\omega_j t}) \tag{163}$$

We need to pass this operators to the continuum. Knowing that the commutation rules should be invariant and that the units of Dirac's Delta $\delta(\omega - \omega')$ are $\frac{1}{\omega}$, the operators are modified as follows

$$\left[\frac{\hat{f}_j}{\sqrt{\delta_{\omega_j}}}, \frac{\hat{f}_j^\dagger}{\sqrt{\delta_\omega}}\right] = \lim_{\delta_\omega \to 0} \frac{\delta_{\omega_j, \omega_{j'}}}{\delta_\omega} = \delta(\omega - \omega'). \tag{164}$$

We define the operators in the continuum as

$$\hat{f}_\omega = \frac{\hat{f}_j}{\sqrt{\delta_\omega}} \tag{165}$$

$$\hat{f}_\omega^\dagger = \frac{\hat{f}_j^\dagger}{\sqrt{\delta_\omega}}. \tag{166}$$

Therefore, the summation can now be written as

$$\sum_j \alpha_j \dot{\hat{x}}_j^h(\mathbf{k}, t) = \sum_j \frac{\delta_\omega}{\delta_\omega} \frac{\sqrt{\mu\omega_j}}{\sqrt{\mu\omega_j}} \alpha_j \dot{\hat{x}}_j^h(\mathbf{k}, t) = \sum_j \delta_\omega \frac{\sqrt{\mu\omega_j}}{\sqrt{\delta_\omega}} \dot{\hat{x}}_j^h(\mathbf{k}, t) \underbrace{\frac{\alpha_j}{\sqrt{\mu\omega_j}\sqrt{\delta_\omega}}}_{\xi}. \tag{167}$$

We shall use the equivalence $\frac{\delta_{ij}}{\delta_\omega} = \delta(\omega_j - \omega_i)$ to work on the ξ expression:

$$\xi^2 = \frac{\alpha_j^2}{\mu\omega_j} \frac{1}{\delta_\omega} = \sum_i \frac{\alpha_i^2}{\mu\omega_i} \frac{\delta_{ij}}{\delta_\omega} = \sum_i \frac{\alpha_i^2}{\mu\omega_i} \delta(\omega_j - \omega_i) = J(\omega). \tag{168}$$

Recalling Eq.(24), we conclude that when $\omega_j \to \omega$, then $\xi^2 \to J(\omega)$.

Using the rectangle rule, $\sum_j \omega_j \cdot \delta_\omega = \int d\omega$, and Eqs.(163), (167) and (168), we finally present the

equation of the summation as an integral:

$$\sum_j \alpha_j \hat{\vec{x}}_j^h(\mathbf{k},t) = \int_0^\infty d\omega \sqrt{J(\omega)}\sqrt{\mu\omega}\, i\sqrt{\frac{\hbar\omega}{2\mu}}(\hat{f}_\omega^\dagger e^{i\omega t} - \hat{f}_\omega e^{-i\omega t}). \tag{169}$$

E Green's Function Review

Green's function is an integral kernel that can be used to solve differential equations [31]. It is specially useful to find the particular solution of a differential equation.

Consider the following inhomogeneous equation:

$$\mathcal{L}\mathbf{B} = \mathbf{D}, \tag{170}$$

where $\mathcal{L}$ is a linear operator acting on the vector field $\mathbf{B}$ representing the unknown response of the system. The vector field $\mathbf{D}$ is a known source function and makes the differential equation inhomogeneous. Usually it is difficult to find a solution of Eq.(170) and it is easier to consider $\mathbf{D}$ to be the special inhomogeneity $\delta(\mathbf{r}-\mathbf{r}')$. Then, the linear equation reads as

$$\mathcal{L}\mathbf{G}_i(\mathbf{r},\mathbf{r}') = \delta(\mathbf{r}-\mathbf{r}') \qquad i=(x,y,z) \tag{171}$$

where $\mathbf{n}_i$ denotes an arbitrary constant unit vector. In general the Green function is dependent on the inhomogeneity position and it is include as one of its arguments [1].

The equations showed in Eq.(171) can be written in a shorter form as

$$\mathcal{L}\overleftrightarrow{G}(\mathbf{r},\mathbf{r}') = \overleftrightarrow{I}\delta(\mathbf{r}-\mathbf{r}'). \tag{172}$$

where the operator $\mathcal{L}$ acts on each column of $\overleftrightarrow{G}$ separately and $\overleftrightarrow{I}$ is the unit dyad. The dyadic function $\overleftrightarrow{G}$ is known as the Dyadic Green's function.

Assuming that Eq.(172) has been solved and $\overleftrightarrow{G}$ is known, the particular solution is found with

$$\mathbf{B}(\mathbf{r}) = \int_V \overleftrightarrow{G}(\mathbf{r},\mathbf{r}')\mathbf{D}(\mathbf{r}')dV', \tag{173}$$

integrating over the volume V in which $\mathbf{D} \neq 0$.

F Coupling Constant Without Disperssion

This appendix aims to prove that the coupling constant between the emitter and the electric field is the same in a medium with and without dissipation. We recall that the electric field in media with absorption is given by the particular solution of Eq.(57) whereas in a medium with $\varepsilon_i = 0$ the electric field is its given by its homogeneous solution.

The interaction Hamiltonian in the dipole approximation is, for both of the cases,

$$-\hat{\sigma}_x\hat{\mathbf{d}}\cdot\hat{\mathbf{E}}(\mathbf{r}_e). \tag{174}$$

This expression was developed in the main text for an absorbing media finishing as

$$\hat{H}_{int} = -\hbar\hat{\sigma}_x\int d\omega g(\omega)(\hat{b}(\omega) - \hat{b}^\dagger(\omega)), \tag{175}$$

where $g(\omega)$ is called the coupling constant.

We now write the interaction Hamiltonian using the expression of the electric field in a non-absorbing

media

$$\hat{H}_{int} = -\hat{\sigma}_x \sum_l i\sqrt{\frac{\hbar\omega_l}{2\varepsilon_0}}(\hat{a}_l e^{-i\omega_l t} - \hat{a}_l^\dagger e^{i\omega_l t})\mathbf{d}\cdot\mathbf{u}_l(\mathbf{r}). \tag{176}$$

Passing this expression to the Fourier space of ω, it reads as

$$\hat{H}_{int} = -\hat{\sigma}_x \sum_l i\sqrt{\frac{\hbar\omega_l}{2\varepsilon_0}}(\hat{a}_l - \hat{a}_l^\dagger)\mathbf{d}\cdot\mathbf{u}_l(\mathbf{r}_e)\delta_{\omega\omega_l}. \tag{177}$$

We can simplify the above equation as

$$\hat{H}_{int} = -\hbar\hat{\sigma}_x \sum_l g_l(\hat{a}_l - \hat{a}_l^\dagger), \tag{178}$$

where it has been included the shorthand notation:

$$g_l = i\sqrt{\frac{\omega_l}{2\hbar\varepsilon_0}}\mathbf{d}\cdot\mathbf{u}_l(\mathbf{r}_e)\ \delta_{\omega\omega_l}. \tag{179}$$

We use the equivalence [1],

$$Im[\overleftrightarrow{G}\ (\mathbf{r}_e,\mathbf{r}_e,\omega)] = \frac{\pi c^2}{2\omega}\sum_l \mathbf{u}_l^*(\mathbf{r}_e)\mathbf{u}_l(\mathbf{r}_e)\delta_{\omega,\omega_l}, \tag{180}$$

to write the coupling constant regarding the dyadic Green function.

$$|g(\omega)|^2 = \frac{\omega^2}{\pi c^2\varepsilon_0\hbar}\vec{d}^T Im[\overleftrightarrow{G}\ (\mathbf{r}_e,\mathbf{r}_e,\omega)]\vec{d} \tag{181}$$

It can be observed that we have got the same equation as Eq.(78). And, so that, both coupling constants are equal.

G Conditions for Strong Regime in a Cavity QED

Having a TLS inside a cavity QED, we describe them, as in the main text through the Spin-Boson model in the RWA with the losses in the media introduced by a spectral density $g(\omega)$ with the form of a Lorentzian function. The Hamiltonian is given by

$$\hat{H}_{eff} = -\hbar\frac{\Delta}{2}\hat{\sigma}_z - \hbar\int d\omega g(\omega)(\hat{a}\hat{\sigma}_+ - \hat{a}^\dagger\hat{\sigma}_-) + \int d\omega\ \omega\hat{a}^\dagger\hat{a}. \tag{182}$$

We want to know how the probability of the excited TLS, $|c_0^e(t)|^2$, evolves with time having the initial conditions $c_0^e(0) = 1$ and $c_g^{1\omega} = 0$ for any ω. The possible states of the emitter along time are given by the wave function

$$|\psi(t)\rangle = c_0^e(t)\,|e,0\rangle + \int d\omega c_{1\omega}^g\,|g,1_\omega\rangle\,, \tag{183}$$

where $c_{1\omega}^g(t)$ are the coefficients of the states with the emitter in the ground state and one photon in a mode ω.

We calculate the evolution of this wave function in the interaction picture through Schrödinger equation

$$|\dot{\psi}(t)\rangle = -\frac{i}{\hbar}H_{int}^I\,|\psi(t)\rangle\,. \tag{184}$$

Here, H_{int}^I is

$$H_{int}^I = \hbar\int d\omega g(\omega)(\hat{a}\hat{\sigma}_+ e^{-i(\Delta-\omega)t} - \hat{a}^\dagger\hat{\sigma}_- e^{i(\Delta-\omega)t}). \tag{185}$$

Therefore, the derivatives with respect to time of the coefficients are

$$\dot{c}_0^e(t) = -i \int d\omega g(\omega) e^{i(\Delta-\omega)t} c_{1\omega}^g(t) \tag{186}$$

$$\dot{c}_{1\omega}^g(t) = -ig(\omega) e^{-i(\Delta-\omega)t} c_0^e(t). \tag{187}$$

In order to get an equation that involves $c_0^e(t)$ only, we first integrate Eq.(186)

$$c_{1\omega}^g(t) = \int dt' - ig(\omega) e^{-i(\Delta-\omega)} c_0^e(t'). \tag{188}$$

On substituting the expression of $c_{1\omega}^g(t)$ in Eq.(186) we obtain

$$\dot{c}_0^e(t) = -\int d\omega |g(\omega)|^2 \int_0^t dt' e^{i(\Delta-\omega)(t-t')} c_0^e(t'). \tag{189}$$

Here, the integral in ω goes from 0 to ∞. However, we know that the shape of $g(\omega)$ is a Lorentzian centred about the atomic transition frequency $\Delta = \Omega > 0$. When we move away from Δ, $g(\omega)$ tends to zero and consequently, the integrand tend to zero. In this way we can extend the integral in ω to $-\infty$ without any change in the result.

Substituting the value of the spectral density,

$$g^2(\omega) = \frac{1}{\pi} \frac{g^2\Gamma/2}{(\Omega-\omega)^2 + \left(\frac{\Gamma}{2}\right)^2}, \tag{190}$$

in Eq.189, we get

$$\dot{c}_0^e(t) = -\frac{1}{\pi} g^2 \frac{\Gamma}{2} \int_0^t dt' \int_{-\infty}^{\infty} d\omega \frac{e^{i(\Delta-\omega)(t-t')}}{(\Delta-\omega)^2 + \frac{\Gamma}{4}} c_0^e(t'). \tag{191}$$

The integral on ω is easy to perform by Cauchy theorem, arriving at

$$\dot{c}_0^e(t) = -\frac{1}{\pi} g(\omega)^2 \int_0^t dt' e^{-\frac{\Gamma}{2}|t-t'|} c_0^e(t'). \tag{192}$$

Deriving all this equation with respect to time (t) by using Leibniz rule, and taking into account that $t > t'$ for all t, we finally find the motion equation of $c_0^e(t)$:

$$\ddot{c}_0^e(t) = -g(\omega)^2 c_0^e(t) - \frac{\Gamma}{2} \dot{c}_0^e(t) \tag{193}$$

This is equivalent to the motion equation of a classical damped harmonic oscillator. Said oscillator is overdamped if $g < \frac{\Gamma}{4}$. In the overdamped regime, the probability of finding the emitter in the excited states decays as a sum of two exponential. The oscillator is underdamped if $g > \frac{\Gamma}{4}$, then the probability of finding the emitter in the upper state is

$$|c_0^e|^2 = A^2 cos^2 \left(\sqrt{\left(g^2 - \frac{\Gamma^2}{16}\right)} t + \phi \right) e^{-\frac{\Gamma}{2}t}, \tag{194}$$

being A and ϕ some constants determined by the initial conditions. These oscillations characterizes the strong regime. Therefore, **we will only observed Rabi oscillator if** $g > \frac{\Gamma}{4}$.

H How to Compute $G_{zz}(\mathbf{0})$

In this appendix we develop techniques to analyse the kernels of

$$G_{zz}(\mathbf{0}) = \underbrace{\frac{ig}{4\pi}\int_0^\infty dq_{||}\frac{q_{||}^3}{q_{az}}}_{G_{zza}(\mathbf{0})} + \underbrace{\frac{-ig}{4\pi}\int_0^\infty dq_{||} r_{am}\frac{q_{||}^3}{q_{az}}e^{2iq_{az}\tilde{h}}}_{G_{zzRam}(\mathbf{0})} \qquad z>0 \tag{195}$$

that enable us to compute the integrals. The variable of integration is the parallel part of the normalized wave vector, $q_{||} = \frac{k_{||}}{g}$. Here $g = \frac{\omega}{c}$, $\tilde{h} = hg$ is the normalized distance from the surface to the emitter, $r_{am} = \frac{q_{mz}-q_{az}\bar{\varepsilon}_m}{q_{mz}+q_{az}\bar{\varepsilon}_m}$ is the reflection factor and q_{az} and q_{mz} are the transversal part of the normalized wave vector in the air and the metal, respectively.

The Cauchy theorem tells that the integrals through two paths which connect the same two points are equal if the function is holomorphic everywhere in between the two paths. The integrands of Eq.(195) are holomorphic everywhere except poles and branch cuts. Our goal is to find a path that connect the points $q_{||}=0$ and $q_{||}=\infty$ that does not have any singularity in the area within this new path and the positive real line. Therefore, in order to obtain the new path, we need to find the poles and branch cuts of the integrands.

Since q is the normalized wave vector $q=\frac{k}{g}$, its modulus is equal to $|q|=\sqrt{\bar{\varepsilon}(\mathbf{r},\omega)}$. When we are working within the air, $\bar{\varepsilon}(\mathbf{r},\omega)=1$, the transversal part q_{az} can be written in terms of the parallel part as

$$q_{az} = \sqrt{1-q_{||}^2} \tag{196}$$

and when we are working in the metal as

$$q_{mz} = \sqrt{\bar{\varepsilon}-q_{||}^2}. \tag{197}$$

The Green function presents two poles, one if $q_{az}=0$ an another if $1/r_{am}=0$. The pole $1/r_{am}=0$ represents the plasmons because it produces a reflected wave even if there is not emitter.

We show the steps to localize a pole focusing on the pole $q_{az}=0$, since the procedure would be similar for $r_{am}=0$. In order to treat the singularity of $q_{az}=\frac{1}{\sqrt{\bar{\varepsilon}-q_{||}^2}}$, we have to take into account the infinitesimally small absorption as follows:

$$\bar{\varepsilon} \to \bar{\varepsilon} + i\delta. \tag{198}$$

We introduce the absorption in this way to prevent that a wave created in the emitter is infinitely large at a position infinitely far from it [21]. As it is shown in Fig.(12), there will be two $q_{||}$ that fulfil the condition $q_{az}=0$.

Since the integral goes from $q_{||}=0$ to $q_{||}=\infty$, we only have to avoid the poles with a positive imaginary part. So far, it looks convenient to do the integral through a path located in the lower-half plane. However, we still need to find the branch cuts to figure out the optimal path.

The kernels in Eq.(195) include multivalued functions as q_{az} and q_{mz}. Although we have already chosen the solution with a positive imaginary part, there are more possible solutions. To explain the concept of a branch cut we utilize the function $w = Im\sqrt{z} > 0$. Being z a complex number $z=re^{i\theta}$, the solution is

$$w = \begin{cases} \sqrt{z}e^{i\theta/2}, & \text{if } \theta \le \pi. \\ \sqrt{z}e^{-i\theta/2}, & \text{if } \theta > \pi. \end{cases} \tag{199}$$

If z moves around the origin in a full circle, $z=re^{i(\theta+2\pi)}$, there are a discontinuity in the value of w when z crosses the real positive axis. This is the definition of a branch cut: a curve in the complex plane across which an analytic multivalued function is discontinuous. The function $w=\sqrt{z}$ presents a branch cut defined

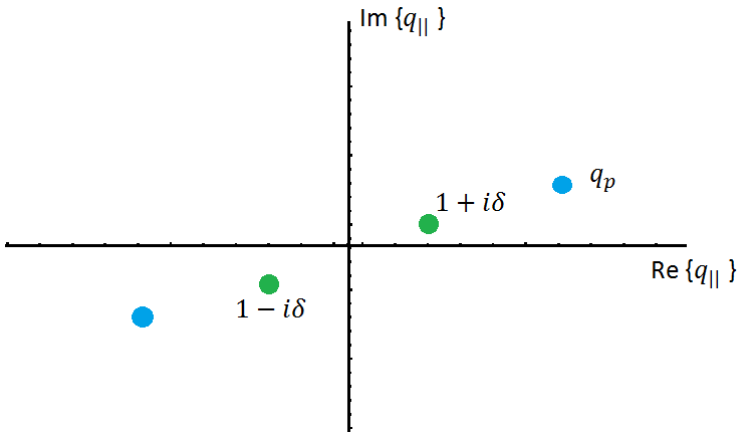

Figure 11: Poles of the integrand of $G_{zzRam}(\mathbf{0})$. The blue points indicate the poles due to the plasmons and the green points the pole in $|q_{||}|= 1$ adding a small absorption.

as:

$$\begin{cases} Im\{z\} = 0, \\ Re\{z\} \geq 0. \end{cases} \tag{200}$$

We can implement this result in q_{az} and q_{mz}, substituting z by

$$z = \bar{\varepsilon} - q_{||}^2. \tag{201}$$

The curve in the complex plane of $q_{||}$ that fulfil $Im\{z\} = 0$ and $Re\{z\} \geq 0$ draws the branch cut. In the case of q_{az}, we need to add a small absorption as $\bar{\varepsilon} \to \bar{\varepsilon} + i\delta$. Its branch cut obeys

$$\delta = Im\{q_{||}\} \cdot Re\{q_{||}\} \tag{202}$$

$$1 + Im\{q_{||}\} - Re\{q_{||}\} \geq 0 \tag{203}$$

with $Re\{q_{||}\} \in [-1, 1]$. For q_{mz} the conditions are

$$\delta = Im\{q_{||}\} \cdot Re\{q_{||}\} \tag{204}$$

$$1 + Im\{q_{||}\} - Re\{q_{||}\} \geq 0 \tag{205}$$

with $Re\{q_{||}\}\epsilon[-\bar{\varepsilon}_R, \bar{\varepsilon}_R]$.

These branch cuts are placed in the upper part of the complex plane of $q_{||}$ [21]. Therefore we can carry out the integral through the path marked in Fig.(13).

Since the kernels of Eq.(195) fall as an exponential when $q_{||}$ increases, we can modify the upper limit of the integral from ∞ to 50, for example. In this way we can neglect the integral through the path parts 2 and 3 [See Fig. (12)].

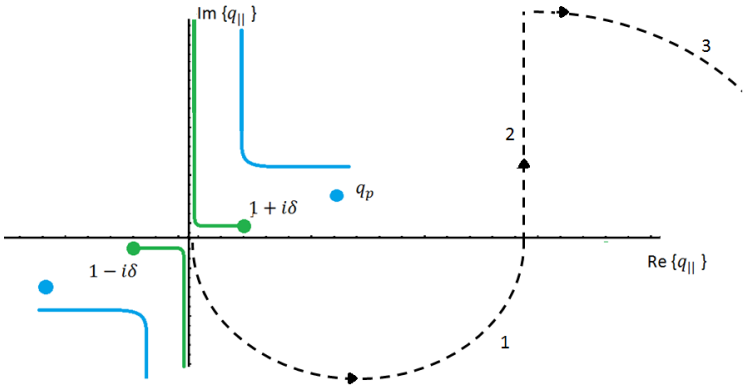

Figure 12: Schema of the poles, branch cuts and path taken to carrying out the integral. The lines and points in green are the branch cut and poles resulting from q_{az} and the ones in blue come from q_{mz}. We do the integral through the dashed path. It has the same result as the integral through the real positive axis because there are not any discontinuity between the two paths.

Code

This appendix presents the codes written in Matlab which were used to solve the integral equal to $Im[G_{zz}(\mathbf{r}_e, \mathbf{r}_e, \omega)]$,see Eq. (195), of an emitter near to a metallic surface of gold or silver.

H.1 Purcell

purcell.m is the main program used to find the Purcell factor.

```
(* ::Package:: *)

%% Input data
%
% distances in microns
%
% metal, 1=silver, 2=gold, 8=tungsten
%
imetal = 2;

 nomega=500;
 delomega=0.005;
 omegain=1.37;
%  delomega=0.0008;
%  omegain=3.4;

 idirdip=3;
% distancias=0.001;
 distancias=0.001:0.001:0.019; % real distances in micrometres
 ndistancias = length(distancias);
 hs = zeros(1,ndistancias); % adimensional distaces
 omegas=zeros(1,nomega);
 epsilontodos=zeros(1,nomega);
%
% Loop in distances
```

```
gamma_0=logspace(7,4,11);% intrinsic decay rate of the emisor in eV
ngamma_0=length(gamma_0);
purcellt = zeros(nomega,ngamma_0);
for idistancias = 1: ndistancias
      dis0 = distancias(idistancias);
     %
     % loop in omegas

      for iomega = 1: nomega


         % vlan0 = vlanin + (ivlan 1) * delvlan;
         % gvaccum0 = 2.d0 * pi / vlan0;

         % omegaev = 1.240 / vlan0;
         omega0=omegain + (iomega 1)*delomega;
         gvaccum0 = 2.d0 * pi*omega0/1.240;
         omegaev=omega0;
         epsmetal = epsilon_metal(imetal, omegaev);
         omegas(iomega)=omegaev;
         epsilontodos(iomega)=epsmetal;
         dis = dis0 * gvaccum0; % normalized distances
         hs(idistancias) = dis; % hs es distancias normalizadas

  % Dipole in Z direction
  %
         if idirdip == 3;
            [imGvac, imGref, imG, N, tvec] = function_purcell_z(dis, epsmetal
                , gvaccum0);

            for igamma_0 = 1: ngamma_0
            % purcellt(iomega,igamma_0) = (gamma_0(igamma_0)*(3/2)*real(imG
                )); % Esto es directamente g^2(w)*2pi in eV
            purcellt(iomega,igamma_0) = real(imG);
            end
            % purcelltA (ivlan)=real (imGref)/real(imGvac)+1;
         end


      end



for icaca = 1: ngamma_0
for iomega = 1: nomega
    % purcellt(iomega,icaca) = purcellt(iomega,icaca)*omegas(iomega)*omegas(
        iomega)*omegas (iomega)/(3.256000*3.256000*3.256000); % Esto es
        directamente g^2(w)*2pi in eV
end
end
%
% end loop in omegas (eV)
```

```
%

%       %
%       % writing out the results


for igamma_0 = 1:ngamma_0
gammita=num2str(igamma_0);
s=num2str(dis0);
s=strcat('Silverdis=',s,'_i=',gammita);


fileID1 = fopen(strcat('C:\Users\usuario\Dropbox\master\TFM\PURCELL_Ag_W (matlab program)\imG\data_files\max\',s,'.txt'),'w');
[M,I] = max(purcellt,[],1);
fprintf(fileID1,'%f ',omegas(I(1)));
fclose(fileID1);

fileID = fopen(strcat('C:\Users\usuario\Dropbox\master\TFM\PURCELL_Ag_W (matlab program)\imG\data_files\',s,'.txt'),'w');
fprintf(fileID,'#  Omega (eV) \t imG   \n');
for iomega = 1:nomega
    fprintf(fileID,'%f \t %.9f \n',omegas(iomega), purcellt(iomega,igamma_0));
end
fclose(fileID);



figure (1)
plot(omegas,real(epsilontodos), 'bx ');
title (s)
s=strcat(s,'.png');
ylabel gamma_0*3/2*imG
xlabel omega(eV)
saveas(1, strcat('C:\Users\usuario\Dropbox\master\TFM\PURCELL_Ag_W (matlab program)\imG\plots\',s), 'png');
end
end
```

H.2 Purcell_function

The main program calls the function *Purcell_function* in which the integral is performed along the complex plane.

```
function [imGvac, imGref, imG, N, tvec] = function_purcell_z(dis, eps, gvaccum0)

        cz = 0;
        ui = 1i;
%
        R = max(10/dis,10); % qmax=10/dis
        N=10000;
```

```
        deltat = pi/N;
%
        tvec=zeros(1,N);
        qpurvac = zeros(1,N);
        purctot = zeros(1,N);
        qpurc = zeros(1,N);
        imGvac = 0;
        imGref = 0;
        imG = 0;
%
        for iq = 1:N
             t= (iq 0.5)*pi/N;
             q=R*(1 cos(t)) R*ui*sin(t);
             qz = cdsqrtnew(1    q^2);
             qz2 = cdsqrtnew(eps    q^2);
             tvec(iq)=qz;
%
            refle = (eps*qz    qz2)/(eps*qz + qz2);
            expo = exp(2*ui*qz*dis);
%

            qpurvac(iq) = ( q^3 / qz);
            purctot(iq) = ( q^3 / qz * refle * expo);
            qpurc(iq) = (q^3 / qz * (1+ refle * expo));
            imGvac = imGvac + R*(sin(t) ui*cos(t))*pi/N* qpurvac(iq);
            imGref = imGref + R*(sin(t) ui*cos(t))*pi/N* purctot(iq);
            imG = imG + R*(sin(t) ui*cos(t))*pi/N*qpurc(iq);
        end


        end
```

H.3 Epsilon_metal

The function epsilon_metal calculates the permittivities of the metals following Eq.(92)

```
function [epsmetal] = epsilon_metal(imetal, omega)
%
% returns the dielectric constant for several metals for an input frequency
% in eV
%
    ui = 1i;
%
    % Silver
    if (imetal ==1);
        epsr = 4.6;
        omegap0 = 9.0;
        lgamma0 = 0.07;
        deltaeps0 = 1.1;
        bomega0 = 4.9;
        bgamma0 = 1.2;
        epsmetal = epsr     omegap0^2/omega/(omega+ui*lgamma0)     ...
```

```
17                          deltaeps0 * bomega0^2/(omega^2 bomega0^2+ui*omega*
                                bgamma0);
18      end
19      % Gold
20      if (imetal ==2);
21          epsr = 5.967;
22          omegap0 = 8.729;
23          lgamma0 = 0.065;
24          deltaeps0 = 1.09;
25          bomega0 = 2.684;
26          bgamma0 = 0.433;
27          epsmetal = epsr    omegap0^2/omega/(omega+ui*lgamma0)    ...
28                          deltaeps0 * bomega0^2/(omega^2 bomega0^2+ui*omega*
                                bgamma0);
29      end
30      % Cooper
31      if (imetal ==3);
32          epsr = 1.;
33          omegap0 = 8.212;
34          lgamma0 = 0.03;
35
36          deltaeps0 = 84.49;
37          bomega0 = 0.291;
38          bgamma0 = 0.378;
39
40          deltaeps1 = 1.395;
41          bomega1 = 2.957;
42          bgamma1 = 1.056;
43
44          deltaeps2 = 3.018;
45          bomega2 = 5.3;
46          bgamma2 = 3.213;
47
48          deltaeps3 = 0.598;
49          bomega3 = 11.18;
50          bgamma3 = 4.305;
51          epsmetal = epsr    omegap0^2/omega/(omega+ui*lgamma0)    ...
52                          deltaeps0 * bomega0^2/(omega^2 bomega0^2+ui*omega*
                                bgamma0)    ...
53                          deltaeps1 * bomega1^2/(omega^2 bomega1^2+ui*omega*
                                bgamma1)    ...
54                          deltaeps2 * bomega2^2/(omega^2 bomega2^2+ui*omega*
                                bgamma2)    ...
55                          deltaeps3 * bomega3^2/(omega^2 bomega3^2+ui*omega*
                                bgamma3);
56      end
57
58      % Tungsten
59      if (imetal ==8);
60          epsr = 1.;
61          omegap0 = 5.955;
62          lgamma0 = 0.027;
```

```
63          omegap1 = 2.286;
64          lgamma1 = 0.335;
65          deltaeps0 = 12.0;
66          bomega0 = 0.984;
67          bgamma0 = 0.590;
68          deltaeps1 = 14.4;
69          bomega1 = 2.066;
70          bgamma1 = 1.653;
71          deltaeps2 = 12.9;
72          bomega2 = 4.132;
73          bgamma2 = 2.479;
74          epsmetal = epsr    omegap0^2/omega/(omega+ui*lgamma0)    ...
75                             omegap1^2/omega/(omega+ui*lgamma1)    ...
76                             deltaeps0 * bomega0^2/(omega^2 bomega0^2+ui*omega*
                                bgamma0)    ...
77                             deltaeps1 * bomega1^2/(omega^2 bomega1^2+ui*omega*
                                bgamma1)    ...
78                             deltaeps2 * bomega2^2/(omega^2 bomega2^2+ui*omega*
                                bgamma2);
79      end
80  end
```